

HbCIPK2, a novel CBL-interacting protein kinase from halophyte *Hordeum brevisubulatum*, confers salt and osmotic stress tolerance

RUIFEN LI, JUNWEN ZHANG, GUANGYU WU, HONGZHI WANG, YAJUAN CHEN & JIANHUA WEI

Beijing Agro-biotechnology Research Center, Beijing Academy of Agriculture and Forestry Sciences, Beijing 100097, China

ABSTRACT

Protein kinases play an important role in regulating the response to abiotic stress in plant. CIPKs are plant-specific signal transducers, and some members have been identified. However, the precise functions of novel CIPKs still remain unknown. Here we report that *HbCIPK2* is a positive regulator of salt and osmotic stress tolerance. *HbCIPK2* was screened out of the differentially expressed fragments from halophyte *Hordeum brevisubulatum* by cDNA-AFLP technique, and was a single-copy gene without intron. Expression of *HbCIPK2* was increased by salt, drought and ABA treatment. *HbCIPK2* is mainly localized to the plasma membrane and nucleus. Ectopic expression of 35S:*HbCIPK2* not only rescued the salt hypersensitivity in *Arabidopsis* mutant *sos2-1*, but also enhanced salt tolerance in *Arabidopsis* wild type, and exhibited tolerance to osmotic stress during germination. The *HbCIPK2* contributed to the ability to prevent K⁺ loss in root and to accumulate less Na⁺ in shoot resulting in K⁺/Na⁺ homeostasis and protection of root cell from death, which is consistent with the gene expression profile of *HbCIPK2*-overexpressing lines. These findings imply possible novel *HbCIPK2*-mediated salt signalling pathways or networks in *H. brevisubulatum*.

Key-words: CIPK; K⁺ homeostasis; salt tolerance.

INTRODUCTION

Soil salinity and drought are critical environment threats to crop development and yield worldwide (Munns & Tester 2008; Møller *et al.* 2009). Improvement of crop salt and drought tolerance is an effective and long-term way to cope with these stresses (Flowers 2004). Therefore, it is a key basis for breeding new stress-tolerant crop cultivars to discover novel important regulators in salt and drought stress responses.

Plant tolerance to salt or drought is a complex multigenic process, in which many genes are involved to respond (Zhu 2002; Shabala & Cuin 2007; Miller *et al.* 2010). Especially,

Correspondence: J. H. Wei. Fax: +86 10 51503830; e-mail: weijianhua@baafs.net.cn

high salinity causes ion toxicity and ion imbalance, generates osmotic stress and second oxidative stress (Hasegawa *et al.* 2000), so molecular mechanisms of salt tolerance in higher plants involve many aspects such as ionic, osmotic and reactive oxygen species (ROS) homeostasis and more, which differ from one species to another (Mian *et al.* 2011). Moreover, cross-talks exist between salt and other stress signalling (Ma, Gong & Bohnert 2006). In this regard, the understanding of the overall ionic and osmotic tolerance mechanisms still remains limited (Munns & Tester 2008).

To date, extensive researches focus on identifying salt-responsive regulators and dissecting salt stress pathways at the cellular, organ and whole-plant level (Ma *et al.* 2006; Munns & Tester 2008). Based on responsive stage, the identified regulators that are involved in salt tolerance can be classified into two categories: (1) early responsive regulators such as transcription factors (Kim *et al.* 2004; Rushton *et al.* 2012), Ca²⁺-sensors and kinases (Liu *et al.* 2000; Guo *et al.* 2001, 2004; Luan *et al.* 2002; Das & Pandey 2010; Fujii, Verslues & Zhu 2011) and phosphatases (Soon *et al.* 2012); and (2) late responsive regulators which are responsible for ion homeostasis (Shi *et al.* 2002; Apse, Sottosanto & Blumwald 2003; Qiu *et al.* 2004; Hall *et al.* 2006; Maathuis 2006; Møller *et al.* 2009; Hauser & Horie 2010; Mian *et al.* 2011), osmotic adjustment (Zhu 2002) and antioxidative defence (Katiyar-Agarwal *et al.* 2006; Miller *et al.* 2010). However, identifying master regulators and salt stress pathways seem more important for understanding of plant salt tolerance and improving crop tolerance to abiotic stress.

Protein kinases play an important role in plant response to stresses, growth and development. CIPK-type kinase [CBL-interacting protein kinase (CIPK)] is a novel plant-specific family of serine-threonine kinases which CBLs specifically target (Shi *et al.* 1999; Liu *et al.* 2000). CBLs [calci-neurin B-like (CBL)], a kind of Ca²⁺ sensors, can perceive stress signals and specifically interact with CIPK to activate CIPK complexes; activated CBL-CIPK regulates the expression and activity of downstream stress effectors (Luan 2009). Recently, many components of CBL-CIPK signalling pathways have been identified, and functions of partial CBL-CIPK network responsive to abiotic stress also have been dissected (Qiu *et al.* 2002; Xu *et al.* 2006; Fuglsang *et al.* 2007; Huang *et al.* 2011). Notably, the SOS pathway, one of the best-characterized signalling pathways, is

specific to salinity. Of these, CIPK24/SOS2 interacting with CBL4/SOS3 mediated the plasma membrane-bound Na^+/H^+ antiporter, SOS1, conferring salt tolerance in root (Kudla, Batistič & Hashimoto 2010). Whereas, CBL10-CIPK24 complex regulates to protect shoot tissue from salt stress (Quan *et al.* 2007). Interestingly, CIPK24 in turn can phosphorylate CBL10, but not CBL4, which is important for CBL10 function in salt tolerance by stabilizing the membrane localization of the CBL10-SOS2 complex (Lin *et al.* 2009; Du *et al.* 2011). CIPK24/SOS2 was also found to interact with nucleoside triphosphate kinase 2 (NDPK2) that is involved in ROS signalling, as well as with CAT2 and CAT3 (Verslues *et al.* 2007). These findings suggested that CIPK24/SOS2 kinase is an important regulatory node in stress signalling network. In addition to SOS components and signalling pathway, other CIPK components or homologs also have been identified to be required for salt tolerance in an SOS-independent manner (Xiang, Huang & Xiong 2007; Tripathi *et al.* 2009; Tsou *et al.* 2012). There is evidence for CIPKs controlling K^+ transporters such as AKT1 (Lee *et al.* 2007). However, the regulation of K^+ homeostasis via the SOS pathway is most poorly understood.

Even though homologs that involve CBL-CIPK signalling have been identified from non-modelling plants, their roles in salt tolerance and molecular mechanisms are not very clear (Li *et al.* 2009). Especially for halophytic grass, which have evolved specific molecular stress-tolerance mechanisms (Oh *et al.* 2009), the understanding of functions of CIPK-type kinases from halophyte in abiotic stress response may highlight stress signalling pathway.

Wild species are very important genetic resources, which provide a solid basis for the introgression or cloning and transformation of agronomically important genes from wild to cultivated cereals (Nevo & Chen 2010). *Hordeum brevisubulatum* (Trin.) Link is one of wild relatives of cultivated barley, also called as wild barley. This species is indigenous to Asiatic areas and especially grows in saline grassland, belonging to halophytic plant. It can provide gene pools for cereals breeding due to its salt and drought tolerance (unpublished data). However, recent researches on *H. brevisubulatum* are only restricted to genetic relationship and evolution with cultivated barley (Komatsuda *et al.* 1999), and few reports focus on identification of regulators in salt stress response from *H. brevisubulatum* and dissecting their functions in stress signalling pathway.

In this study, we identified *HbCIPK2*, a novel member of CIPK family, from halophytic grass *H. brevisubulatum*, and explored its functions for ionic and osmotic homeostasis in *Arabidopsis*. We also investigated the changes of ion content and flux, salt-induced cell death and gene expression profile by overexpression of *HbCIPK2*, and analysed the possible regulatory mechanism of *HbCIPK2* in salt tolerance. Our data suggest that *HbCIPK2* is required for salt tolerance and may act as salt-triggered signal transducer to mainly regulate K^+ transport in salt stress signalling.

MATERIALS AND METHODS

Plant materials and growth conditions

Seeds of *H. brevisubulatum* used were collected from the saline grassland in Inner Mongolia of China, and immersed in sterilized water for 24 h, then sown in Petri dish (9 mm) with nylon mesh on the top of wet filter papers. After germination, the nylon mesh in which the seedlings have rooted was transferred on the top of container (diameter: 9 mm; height: 13 mm) containing half-strength Hoagland's nutrient solution [major nutrients: 0.4 $\text{NH}_4\text{H}_2\text{PO}_4$, 2.4 KNO_3 , 1.6 $\text{Ca}(\text{NO}_3)_2$, 0.8 MgSO_4 ; micronutrients: 0.1 Fe-chelate, 0.023 $\text{B}(\text{OH})_3$, 0.0045 MnCl_2 , 0.0003 CuCl_2 , 0.0015 ZnCl_2 ; 0.0001 MoO_3 ; all concentrations in units of millimoles per L], and the roots reach into the solution. The plants were grown at 22 °C with a 16 h light/8 h dark photoperiod and an irradiance of 120 $\mu\text{mol m}^{-2} \text{s}^{-1}$. For treatments, solid NaCl or PEG6000 or ABA was added to the growth solution to make the indicated concentration of stress.

The *Arabidopsis* wild type (WT) was referred to *Arabidopsis thaliana* ecotype Columbia; seeds of *Arabidopsis* mutant *sos2-1* described in detail (Liu *et al.* 2000) were ordered from the Arabidopsis Biological Resource Center (ABRC, Ohio; <http://www.arabidopsis.org/abrc/>; stock No. CS3863). Seeds of WT, *sos2-1* and transgenic plants were surface sterilized and sown on Murashige and Skoog (MS) plate following the protocols previously published (Guo *et al.* 2004). Plants were grown either on MS plate or in soil under a 14/10 h light/dark cycle at 21–22 °C with an irradiance of 120 $\mu\text{mol m}^{-2} \text{s}^{-1}$. The relative humidity was approximately 70% ($\pm 5\%$).

Identification of differentially expressed gene *HbCIPK2* by cDNA-AFLP

Total RNA was extracted from the roots of *H. brevisubulatum* seedlings untreated and treated with 430 mM NaCl for 30 min upon the emergence of the third shoot grown in hydroponics using TRIzol reagent (Invitrogen, Carlsbad, CA, USA), then followed by the removal of genomic DNA contamination using Ambion's DNA-free kit (Promega, Madison, WI, USA), and double-stranded cDNA was synthesized according to the manufacturer's instructions for SMART™ cDNA Library Construction Kit (BD Biosciences Clontech, Palo Alto, CA, USA). Differentially expressed fragments (DEFs) were screened using cDNA-AFLP technique according to the procedures as described previously (Bachem, Oomen & Visser 1998). After sequencing, database searches were performed using the BLAST Network Service (NCBI, National Center for Biotechnology Service) (<http://www.ncbi.nlm.nih.gov/BLAST>). One significantly DEF was selected to amplify the full-length cDNA due to the highest nucleotide identity with the sequences of putative serine/threonine proteins in GenBank database. The full-length cDNA of this gene was obtained using the SMART RACE cDNA Amplification Kit (BD Biosciences Clontech). The 5' and 3' nested PCR

primers are listed in Supporting Information Table S1. The amplified RACE products were purified and cloned into the pGEM-T Easy Vector (Promega) to sequence. After assembly of the gene cDNA, the complete coding region of the cDNA and the genomic DNA were amplified using the specific primer pairs listed in Supporting Information Table S1. The PCR conditions were as follows: an initial denaturation at 94 °C for 3 min, followed by 30 cycles at 94 °C for 30 s, 58 °C for 30 s, 72 °C for 1 min and a final extension at 72 °C for 10 min. This gene was designated as *HbCIPK2*.

Bioinformatics analysis of *HbCIPK2* gene

A PSI-BLAST search for *HbCIPK2* homologs was performed using the NCBI BLAST server. Multiple sequence alignment was performed using the program ClustalX1.83. Conserved domains of *HbCIPK2* were predicted using Prosite online software (<http://au.expasy.org/tools/scanprosite>), and a phylogenetic tree was generated with the amino acid sequences of *HbCIPK2* and *Arabidopsis* CIPK proteins using MEGA4 (Tamura *et al.* 2007), with 1000 bootstrap replications. A structure search for *HbCIPK2* was carried out using the TMPRED server (http://www.ch.embnet.org/software/TMPRED_form.html) and TMHMM2.0 server (<http://www.cbs.dtu.dk/services/TMHMM-2.0/>).

Southern blot and Northern blot assays

Genomic DNA was extracted from the three-leaf stage seedlings of *H. brevisubulatum* grown in hydroponics using the CTAB method (Murray & Thompson 1980). For Southern blot analysis, 100 µg of DNA was digested with an excess amount of restriction enzymes such as *Hind*III, *Eco*RI, *Kpn*I, *Pst*I. The digested DNA fragments were separated by electrophoresis on 0.8% (w/v) agarose gel and transferred into a hybond-N⁺ nylon membrane (Amersham Pharmacia Biotech, Piscataway, NJ, USA). To produce a probe, a 650 bp fragment (containing the 350-bp 3' coding region and 150 bp 3' UTR region of the *HbCIPK2*) was amplified with the primers in Supporting Information Table S1 and labelled with DIG-dUTP using PCR Dig probe synthesis Kit (Roche Applied Science, Indianapolis, IN, USA) following the manufacturer's recommendations.

For Northern blot analysis, *H. brevisubulatum* seedlings grown in hydroponics upon the emergence of the third leaf were sampled at the stress point time (1, 3, 6, 12 or 24 h) in the treated conditions (350 mM NaCl, 15% PEG6000 and 50 µM ABA) or untreated condition, and total RNA from *H. brevisubulatum* was extracted using TRIzol reagent (Invitrogen). As for Northern blot analysis of *Arabidopsis* transgenic plants, the transgenic and the control seedlings grown on vertical MS agar plates were collected to extract total RNA. Total RNA from either *H. brevisubulatum* (40 µg) or *Arabidopsis* (20 µg) was fractionated in 1.2% (w/v) denaturing formaldehyde agarose gel, blotted onto nylon membranes (Amersham Pharmacia Biotech). For

HbCIPK2 expression in *H. brevisubulatum*, the probe was the same as that in Southern blot assay. For *HbCIPK2* expression in *Arabidopsis*, a 500 bp cDNA fragment in the 3' region of the *HbCIPK2* open reading frame (ORF) was amplified to use as a probe.

The membrane hybridization and detection were performed following the kit manual (DIG Detection Starter Kit II, Roche Applied Science). The hybridization signals were imaged with *in vivo* imaging system Fujifilm LAS-4000 (Fujifilm, Tokyo, Japan).

Subcellular localization

To make GFP-tagged *HbCIPK2*, the coding regions of *HbCIPK2* was amplified with the primers containing *Bam*HI and *Kpn*I restriction sites, and the PCR product was first cloned into pGEM-T Easy vector (Promega), then sequenced. The ORF of *GFP* was also amplified with the corresponding primer pairs and digested with *Kpn*I and *Sac*I. The digested fragment was inserted into the construct pGEM-T Easy-*HbCIPK2*, and *HbCIPK2* was fused in-frame with the N-terminus of the GFP in the backbone of pGEM-T Easy vector. To construct *AtCBL1n-mRFP*, *AtCBL1n-mRFP* was generated by using a forward primer binding to the mRFP 5' ORF with an extension at the 5' end comprising the first 36 nucleotides of *AtCBL1* (Batistič *et al.* 2008, 2009) and a normal reverse primer of mRFP, which contained *Bam*HI and *Kpn*I restriction sites. All fusion frames were inserted into pGreen0029-35S binary vector (Hellens *et al.* 2000; <http://www.pgreen.ac.uk/>), respectively. For *HbCIPK2*ΔTM-GFP, *HbCIPK2*ΔTM was first amplified by deletion of a transmembrane helix domain located between amino acid residues 196 and 213 of *HbCIPK2* to form the truncated fragment, after sequencing *HbCIPK2*ΔTM replaced *HbCIPK2* in *HbCIPK2*-GFP construct by the restriction sites *Bam*HI and *Kpn*I. The constructs *HbCIPK2*-GFP and *AtCBL1n-mRFP* were co-bombarded while *HbCIPK2*ΔTM-GFP was bombarded alone into onion (*Allium cepa*) epidermal cells according to the method as described (Yokoi *et al.* 2002). Fluorescence detection was performed with a Nikon inverted fluorescence microscope TE2000-E equipped with a Nikon D-Eclipse A1 spectral confocal laser scanning system (Nikon, Tokyo, Japan) 24 h post-transformation. During detection of co-localization, the epidermal peels were treated by 50% sucrose to induce plasmolysis. GFP was examined using an argon laser at 488 nm, for RFP, excitation at 543 nm. All primers were listed in Supporting Information Table S1.

Genetic transformation of *A. thaliana*

To construct the vector used for overexpression of *HbCIPK2*, the ORF of *HbCIPK2* was amplified with the primer pairs and linked into pGEM-T Easy vector (Promega); after sequencing, the construct pGEM-T-*HbCIPK2* was digested with *Bam*HI and *Eco*RI, and inserted into the corresponding sites of a pGreen0029-35S

binary vector. The recombinant plasmid was electroporated into *Agrobacterium tumefaciens* Gv3101 plus pSoup plasmid. The transformation of *Arabidopsis* WT and mutant *sos2-1* was carried out by the floral dip method (Clough & Bent 1998). The seeds of T₀ transformants were harvested and sown on MS medium containing kanamycin (50 mg L⁻¹); the resistant seedlings were transferred in potting soil mixture (rich soil : vermiculite = 2:1, v/v); the positive transgenic plants were further confirmed by amplification of *HbCIPK2* gene or Northern blotting. After two or three generations, homozygous transgenic lines were selected for further analysis.

Identification of transgenic phenotype

To test the salt or osmotic stress tolerance of the transgenic lines, the germination assays were first performed. At least 60 seeds of each transgenic or control *Arabidopsis* line were sterilized and sown on MS plate (1% phytigel and 2% sucrose, w/v, pH 5.7) supplemented with different concentrations of NaCl (125, 150 or 175 mM) and mannitol (300, 350 or 400 mM). The plates were kept at 4 °C for 2 d and then incubated in a growth room at 21–22 °C. After germination for 7 d, the seeds that developed green cotyledons were scored. For seedling growth assays, 7-day-old seedlings each from the WT, the *sos2-1* mutant and the transgenic lines growing on vertical MS plate were transferred onto MS or MS supplemented with different concentrations of NaCl and mannitol described previously, and placed vertically. After growing for 2 weeks, 10 seedlings from each line were weighed, and seedling fresh weight was calculated. For salt tolerance of *HbCIPK2*-overexpressing transgenic lines at reproduction stage, plants were grown in potting soil mixture and kept in growth chambers at 21–22 °C with illumination at 120 μmol m⁻² s⁻¹ for a 14 h daily light period. Half of 3-week-old plants were subjected to salt stress with a final concentration of 250 mM NaCl by the addition of 50 mM increases every 2 d in order to avoid salt shock. The rest plants were irrigated with the same volume of water as control. After stress for 7 d, the developed bolts were recorded and imaged. All assays were repeated three times and the error bars indicated the standard deviation (SD).

Ion content measurements

Ten-day-old seedlings grown on vertical MS plates were transferred onto MS plates without or with 100 mM NaCl, and placed vertically. After growing for 10 d, the shoots and roots were collected, respectively, and washed three times with ddH₂O, and then weighed after drying at 80 °C for 3 d. Approximately 60 mg of samples was digested in 1 mL concentrated HNO₃ at room temperature overnight, then added 2 mL H₂O₂ (30%) and heated at 140 °C for 4 h. After acid digestion, HNO₃ and H₂O₂ were removed through heating at 130 °C; the digested samples were diluted to a total volume of 25 mL with ddH₂O and transferred into new tubes before analysis using an inductively coupled plasma atomic emission spectrometer (ICP-AES).

Ion flux assays

Net fluxes of K⁺ or H⁺ were measured noninvasively using the scanning ion selective electrode technique (SIET) using the SIET system (BIO-001B, Younger USA Sci. & Tech. Corp., Amherst, MA, USA). Microelectrodes were filled with different cocktails by Xuyue Science and Technology Cooperation Limited, essentially as described (Sun *et al.* 2009).

To measure ion fluxes, 5-day-old seedlings of the transgenic, WT or mutant *sos2-1 Arabidopsis* grown on vertical MS plates were transferred into Petri dish (35 mm) containing or without 75 mM NaCl for 30 min, then balanced in measuring buffer (0.1 mM KCl, 0.1 mM CaCl₂, 0.1 mM MgCl₂, 0.5 mM NaCl, 0.2 mM Na₂SO₄, 0.3 mM MES, pH 5.5) for 15 min. Net ion fluxes were measured from the root epidermis in meristematic (about 120 μm from the tip) zones. The ion flux was calculated using the SIET software Mageflux (Younger USA Sci. & Tech. Corp.). All assays were repeated at least three times and the error bars indicated the SD.

Imaging of Na⁺ and salt-induced cell death by fluorescent dyes

To visualize Na⁺ ions, 5-day-old seedlings grown on vertical MS plates were transferred onto MS plates without or with 125 mM NaCl, and placed vertically. After growing for 1 or 2 d, at least 10 seedlings of each line were incubated with 5 μM CoroNa-Green AM (Invitrogen) in liquid MS medium for 2 h. After incubation with CoroNa-Green AM, the seedlings were washed with ddH₂O for three times and stained for 30 min with 1 μg mL⁻¹ propidium iodide (Invitrogen), which is specific dye for dead cells. The roots of stained seedling were cut and observed using confocal laser scanning system (Nikon) at excitation and emission wavelengths of 488 and 516 nm, respectively.

Microarray analysis

Ten-day-old seedlings of the transgenic, WT or mutant *sos2-1 Arabidopsis* grown on vertical MS plates were treated by immersing the roots in MS nutrient solution supplemented without or with 150 mM NaCl for 12 h. More than 30 seedlings of each line were pooled for total RNA isolation with Trizol reagent (Invitrogen), and total RNA was purified using the RNeasy mini kit (Qiagen, Valencia, CA, USA), then confirmed by Agilent 2100 instrument (Agilent Technologies, Santa Clara, CA, USA). Three biological replicates of total RNA were prepared from each line. Agilent Arabidopsis 4 × 44K oligoarrays (Agilent Technologies) were employed for one-color oligoarrays in this study. Probe labelling, hybridization and data analysis were performed by the company as previously described (Zhu *et al.* 2009). The average signals of replica were used for analysis and applied to find the candidate target genes.

Quantitative real-time PCR analyses

To confirm expression of the candidate target genes selected from microarray data, qRT-PCR was performed. Three biological replicates of total RNA from *Arabidopsis* WT, *sos2-1* and transgenic lines under salt stress of 150 mM NaCl for 12 h were reverse transcribed according to the Superscript III kit (Invitrogen). The qPCR was carried out using FastStart Universal SYBR Green Master (Roche Applied Science) on a Roche LightCycler 480 II Real-Time PCR System. The PCR conditions were 95 °C for 15 min followed by 40 cycles at 95 °C for 10 s and 60 °C for 30 s. For every experiment, 5 µL of diluted cDNA solution was used for PCR amplification in a 25 µL volume reaction containing 12.5 µL of FastStart Universal SYBR Green Master and 200 nM of each primer. All experiments were performed in 96-well optical reaction plates with MicroAmp optical adhesive film. The specificity of the amplifications was first confirmed by the presence of a single band of expected size for each primer pair in agarose gel (2% w/v) and then validated by melting curve analysis. The $2^{-\Delta\Delta Ct}$ method was used to calculate the relative gene expression (Livak & Schmittgen 2001). Genes *18S rRNA* and *TUA6* were chosen as internal references, and their expression levels were compared between different samples through experiments; due to the stable expression, *18S rRNA* was used to calculate the relative expression of target genes instead of *TUA6*. Primers used for qPCR analyses were designed using Primer3 (<http://frodo.wi.mit.edu/>), and sequences of specific primers for each selected gene are listed in Supporting Information Table S1.

RESULTS

Identification of differentially expressed gene *HbCIPK2* by cDNA-AFLP

To obtain salt stress responsive regulators, the DEFs were identified using cDNA-AFLP (cDNA-Amplified Fragment Length Polymorphism) from the roots of halophyte *H. brevisubulatum* untreated and treated with 430 mM NaCl for 30 min. Three hundred forty-five DEFs were screened out, among which 110 DEFs were significantly up-regulated (Fig. 1). DEFs with the size of 200–600 base pair were selected to re-amplify and sequence. After sequencing database searches were performed using the BLAST Net-work Service (NCBI) (<http://www.ncbi.nlm.nih.gov/BLAST>). One fragment of DEF1916 showed higher nucleotide identity with the sequences of putative serine/threonine proteins in GenBank database. We utilized the SMART RACE technique to get the full-length cDNA (data not shown).

DEF1916 full-length cDNA is 1689 nt long, with an ORF of 1359 nt that encodes a protein of 452 amino acids with a predicted molecular mass of 51 kDa and isoelectric point of 9.51. Blast search showed that DEF1916 coding sequence shared higher similarity with the ones of plant calcineurin B-like-interacting protein kinases (CIPKs). AtCIPK2 is its

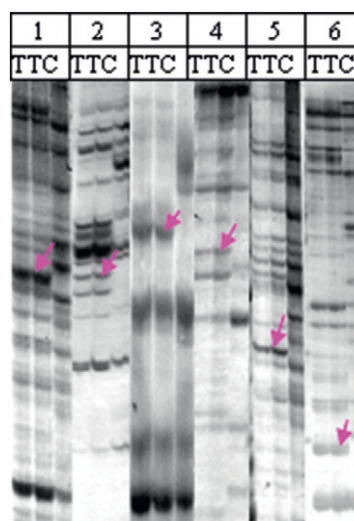


Figure 1. Differentially expressed fragments were screened out by cDNA-AFLP. Letters C and T represent amplified templates from cDNA of *H. brevisubulatum* roots untreated and treated with 430 mM NaCl for 30 min, respectively. The numbers 1–6 indicate different primer pair combination. Arrows show up-regulated bands.

orthologs among *Arabidopsis* 26 CIPK members (Weinl & Kudla 2009) showing 59% sequence identity, while OsCIPK2 is the closest homolog in rice (84%). Hence, this gene is designated as *HbCIPK2* (Accession No. JN831652), a novel member of plant CIPK gene family.

Molecular characterization and expression pattern of *HbCIPK2*

To further characterize *HbCIPK2*, database search together with bioinformatics analysis led to the identification of closer *HbCIPK2* homologs from different plant species (Fig. 2a). A search using Prosite online (<http://au.expasy.org/tools/scanprosite>) and multiple sequence alignment revealed that the deduced *HbCIPK2* contained two domains, an N-terminal highly conserved kinase domain and the C-terminal regulatory domain, and an activation loop was present in the kinase domain, FISL domain (Guo *et al.* 2001) in the regulatory domain (Fig. 2b). The trans-membrane helix domain of *HbCIPK2* was predicted by TMHMM2.0 program, which was located between amino acid residues 196 and 213 (Fig. 2c), just implying as hydrophobicity blot (Fig. 2d). Phylogenetic analysis of *HbCIPK2* with *Arabidopsis* CIPK family indicated that *HbCIPK2* is clustered into the subgroup without intron, and this result also revealed that *HbCIPK2* is closer to AtCIPK2 rather than AtCIPK24 (Fig. 3).

To confirm whether *HbCIPK2* has no intron in *H. brevisubulatum* genome, we amplified *HbCIPK2* from cDNA and genomic DNA. The sequencing result indicated that *HbCIPK2* harbours no intron (data not shown). Southern blot analysis suggested *HbCIPK2* is likely to exist as one copy in the *H. brevisubulatum* genome (Fig. 4a).

(a) HbCIPK2 : -----MGEQKGN--ILMHKYEMGKMLGQGTFAKVYHARNIETSSVSAIKVTDKDKVMKGGITDQVKREISVMKLVKHPN : 72
 OsCIPK2 : -----MAEQRGN--MLMKKYEMGKLLGQGTFAKVYHARNITSSVSAIKMTDKDKVVKGGIMDQIKREISVMKLVKHPN : 72
 ZmCIPK15 : MHACKMMAGHNKRNIILMHKYEMGRLLGQGTFAKVYHARNITRTSSVSAIKVTDKDKVVKVGLVDQIKREISAMKLVKHPN : 80
 SbCIPK25 : -----MVEHKGN--VLMHKYEMGKLLGQGTFAKVYHARNITSSVSAIKVTDKDKVMKVGILIDQIKREISVMKLVKHPN : 72
 AtCIPK2 : -----MENKPS--VLTERRYEVGRLLGQGTFAKVYSGRSNHTNESVSAIKMTDKDKVMRVLGSLQDQIKREISVMRIKHPN : 71

HbCIPK2 : IVQMLEVMATKTKIYFVLEHVKGGELFNKVGQRGLKEDAAKRYFQQLICAVDFCHSRGVYHRDLKPEENLLLDNSNLKVS : 152
 OsCIPK2 : IVQMLEVMATKTKIYFVLEHVKGGELFNKVGQRGLKEDAAKRYFQQLICAVDFCHSRGVYHRDLKPEENLLLDNSNLKVS : 152
 ZmCIPK15 : VVQMLEVIATKTKIYFVLEHVKGGELLAKVQRGLKEDAAKRYFQQLICAVDFCHSRGVYHRDLKPEENLLLDNSDLKVS : 160
 SbCIPK25 : IVQMLEVMATKTKIYFVLEHVKGGELFNKVGQRGLKEDAAKRYFQQLICAVDFCHSRGVYHRDLKPEENLLLDNSNLKVS : 152
 AtCIPK2 : VVQMLEVMATKSRIYFVLEHVKGGELFNKVAKGLKEDAAKRYFQQLICAVDFCHSRGVYHRDLKPEENLLLDNSNLKVS : 151

Activation loop

HbCIPK2 : DFGLSTIIECRRLDGLLHTSCGTPAYVAPEVINRKGYDGAKADIWSCGVILFVLLAGYLPFDKKNLMMYKIKGAEFKC : 232
 OsCIPK2 : DFGLSALIDCRDGLLHTTCGTPAYVAPEVINRKYDGAKADIWSCGVILFVLLAGYLPFDKKNLMMYKIKGAEFKC : 232
 ZmCIPK15 : DFGLSALIECRDGLLHTTCGTPAYVAPEVINRKGYDGAKADIWSCGVILFVLLAGYLPFDKKNLIDLYKIKGAEFKC : 240
 SbCIPK25 : DFGLSALIECRDGLLHTTCGTPAYVAPEVINRKGYDGAKADIWSCGVILFVLLAGYLPFDKKNLMMYKIKGAEFKC : 232
 AtCIPK2 : DFGLSALIDCRDGLLHTTCGTPAYVAPEVINRKYDGAKADIWSCGVVLFVLLAGYLPFDKKNLMMYKIKGAEFKC : 231

* * *

HbCIPK2 : PSWFSSDIRRLLRILDPNPSSTRISIEPRIMEHPWFRKGLDAK--LLRYNLOAKDAVPAADMTVTSDSPSSNSNAIECKEQ : 310
 OsCIPK2 : PSWFNTDVRRLLRILDPNPSSTRISMFKIENPFRKGLDAK--LLRYNLOPKDAIPVDMSTDFDSFN--SAPTE---- : 304
 ZmCIPK15 : PTWFSTHVRRLLRILDPTEGTRISIEPKIENPFRKGLDANLHLLRYNLTNDAPQVDTDKNEDFDPSPSINITDTSKQE : 320
 SbCIPK25 : PSWFSTDARRLLRILDPNPSSTRISMFKIENPFRKGLDAK--LLRYNLOSKNAPQVD--KNADSDSLINITAEKQQ : 308
 AtCIPK2 : PSWFAPEVWRLLCKMLDPNHETRITIAKIESSWFRKGLHLK----QKKMEKMEKQOVR--EATNPMEEAGG--GQNGENH : 306

FISL motif

HbCIPK2 : EAKKLSNLNADFIIIS--LSNGLDLSCMFEEDNKKRESKFTSTNSASTIVSKIEDIAGMRLKLVKDKGMLKMEGSKPGRK : 389
 OsCIPK2 : --KKPSNLNADFIIIS--LSTGLDLSGMFEESDKK--ESKFTSTNSASTIIISKIEDIAGLRLKLVKDKDGLLKMEGSKPGRK : 380
 ZmCIPK15 : DEKKPANMNADFIIISHLSSGLDLSGLFOESDKKTEESKFTSTNTSSAIIISKIEDIADLRLKLVKDKDGLLKMEGSKPGRK : 400
 SbCIPK25 : EEKPTNMNADFIIIS--LSTGLDLSGLFEESDNKREYKFTSTNTSSIVSKIEDVAKNLRKLVKDKDGLLKMEGSKPGRK : 387
 AtCIPK2 : EPPRLATLNADFIIIA--LSTGFGLAGLFGDVYDKRESREASQKPAEELIISKLVEVAKCLKLVKIRKQAGLFLKLERVKEGKN : 385

HbCIPK2 : GVMGIDAEIFEVTPDFHLVELKKTNGDTLEYQRVLENOEMRPALKDIVWAWQGEQPKQEQQQPC----- : 452
 OsCIPK2 : GVMGIDAEIFEVTPDFHLVELKKTNGDTLEYQRVLENOEMRPALKDIVWAWQGEQPKQEQQQPTC----- : 443
 ZmCIPK15 : GVMRIDAEIFEVSPNDFHLVEIKKTNGDTLEYQKVMHNOEMRPALKDIVWAWQGEQLKQEQEQQQ----- : 463
 SbCIPK25 : GVMGIDAEIFEVSPNDFHLVEIKKTNGDTLEYQRVLENOEMRPALKDIVWAWQGEQSKQEQQMI----- : 449
 AtCIPK2 : GILTMDAEIFQVTPDFHLVEVKKKNGDTMEYQKLVEDLRLPALADIVWAWQGEKKEKELQLLQDEQGEQEPS : 456

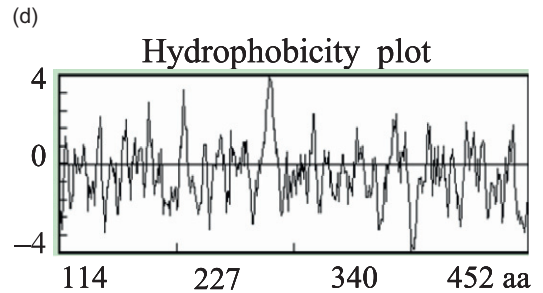
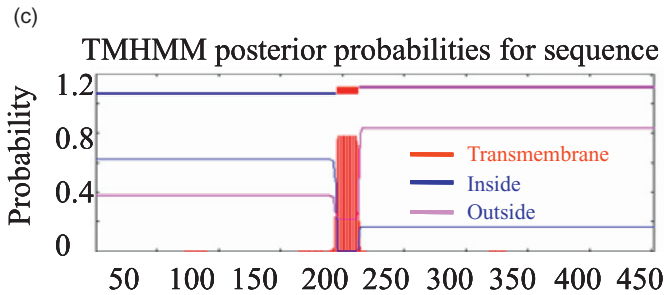
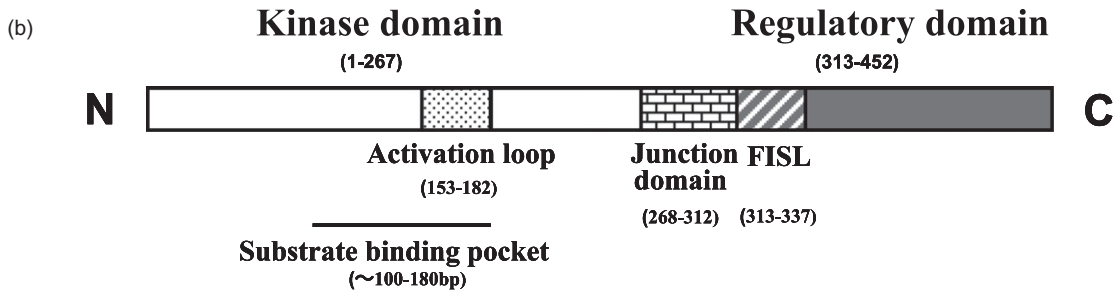


Figure 2. The deduced amino acid sequence alignment, domain prediction and structure analysis of HbCIPK2. (a) Peptide alignment of HbCIPK2 with closer homologs from *Arabidopsis*, rice, maize and sorghum. Black shadings indicate identical residues; grey shadings represent similar residues. The activation loop and FISL motif were shown in N-terminal kinase and C-terminal regulatory domain, respectively. Three highly conserved residues (Thr, Tyr and Ser) are marked with asterisk in the activation loop. Sequences used: SbCIPK25 (ACQ83494), AtCIPK2 (AAF86506), OsCIPK2 (ACD76974), ZmCIPK15 (NP_001148053). (b) Schematic diagram of the domain structure of HbCIPK2. The position of the domains indicated by the numbers was determined by comparing the complete sequence of HbCIPK2 with the domain consensus sequence of all *Arabidopsis* CIPK proteins. (c) The transmembrane helix domain of HbCIPK2 was predicted by TMHMM2.0 program, which was located between amino acid residues 196 and 213. (d) Hydrophobicity blot of HbCIPK2 was carried out using the TMPRED server (http://www.ch.embnet.org/software/TMPRED_form.html).

Expression pattern of *HbCIPK2* in *H. brevisubulatum* seedlings was monitored by RNA gel blot analysis (Fig. 4b). Under 350 mM NaCl stress, the transcripts of *HbCIPK2* began to increase at 1 h after treatment, and then significantly accumulated up from 3 to 24 h. To mimic drought stress, the seedlings were treated by 15% PEG6000. *HbCIPK2* responded slightly to PEG6000 at 1 h, but was dramatically induced from 3 to 12 h, and began to reduce a little at 24 h. For 50 μ M ABA stress, the expression level of *HbCIPK2* was strongly induced. Taken together, these data

support evidence that *HbCIPK2* is up-regulated in response to salt, drought and ABA stress, suggesting that *HbCIPK2* may play an important role in response to salt and drought stress.

To test the localization of HbCIPK2 in plant cells, HbCIPK2-GFP translational fusion was constructed in which GFP was added to the C-terminus of HbCIPK2; another chimeric construct, AtCBL1n-mRFP, was

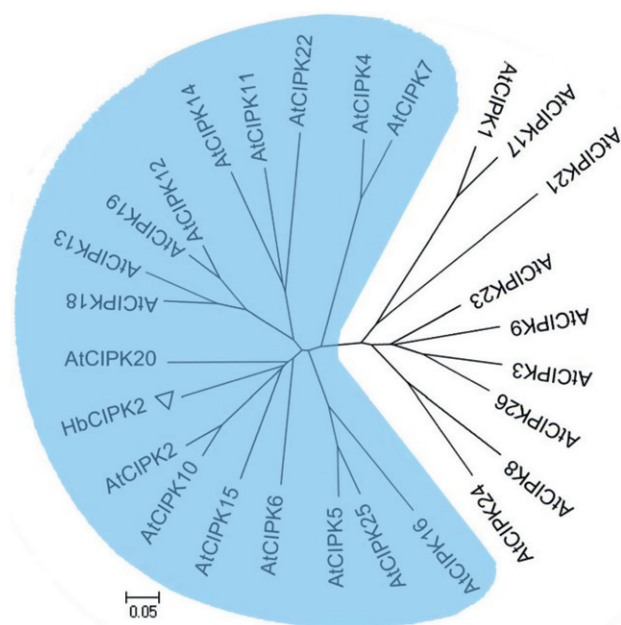


Figure 3. Phylogenetic analysis of HbCIPK2. Phylogenetic relationships of HbCIPK2 with *Arabidopsis* CIPKs. The tree was generated with amino acid sequences of HbCIPK2 and *Arabidopsis* CIPK proteins using MEGA4, with 1000 bootstrap replications. The subgroup of CIPK not harbouring intron sequences is depicted on blue background. The accession number for 26 AtCIPKs: AtCIPK01 (AAG28776), AtCIPK02 (AAF86506), AtCIPK03 (AAF86507), AtCIPK04 (AAG01367), AtCIPK05 (AAF86504), AtCIPK06 (AAF86505), AtCIPK07 (AAK16682), AtCIPK08 (AAK16683), AtCIPK09 (AAK16684), AtCIPK10 (AAK16685), AtCIPK11 (AAK16686), AtCIPK12 (AAK16687), AtCIPK13 (AAK16688), AtCIPK14 (AAK16689), AtCIPK15 (AAK16692), AtCIPK16 (AAK50348), AtCIPK17 (AAK64513), AtCIPK18 (AAK59695), AtCIPK19 (AAK50347), AtCIPK20 (AAK61493), AtCIPK21 (AAK59696), AtCIPK22 (AAL47845), AtCIPK23 (AAK61494), AtCIPK24 (AAK72257), AtCIPK25 (AAL41008) and AtCIPK26 (NP_850861).

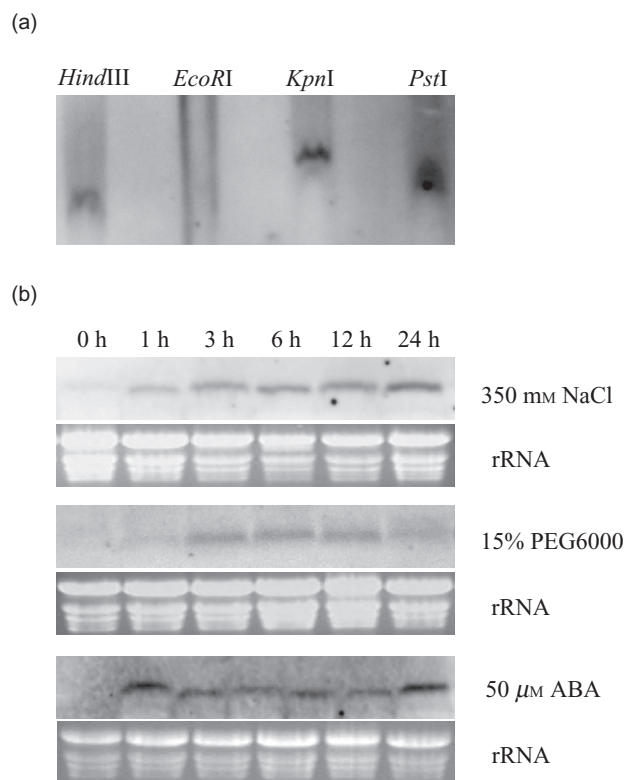


Figure 4. Southern blot analysis and expression pattern of HbCIPK2 in *H. brevisubulatum*. (a) Genomic Southern blot analysis of *HbCIPK2*. Genomic DNA (100 μ g) was digested with *Hind*III, *Eco*RI, *Kpn*I and *Pst*I, respectively. The blot was hybridized with the probe of a 650 bp fragment containing the 350 bp 3' coding region and 150 bp 3' UTR region of the *HbCIPK2* labelled with DIG-dUTP. (b) RNA gel blot analysis of *HbCIPK2* in *H. brevisubulatum*. Total RNA (40 μ g) from *H. brevisubulatum* seedlings without or with the treatment of 350 mM NaCl, 15% PEG6000 and 50 μ M ABA were separated, blotted and hybridized with the same probe as 'Southern blot'; ethidium bromide-stained rRNA bands were shown as a loading control.

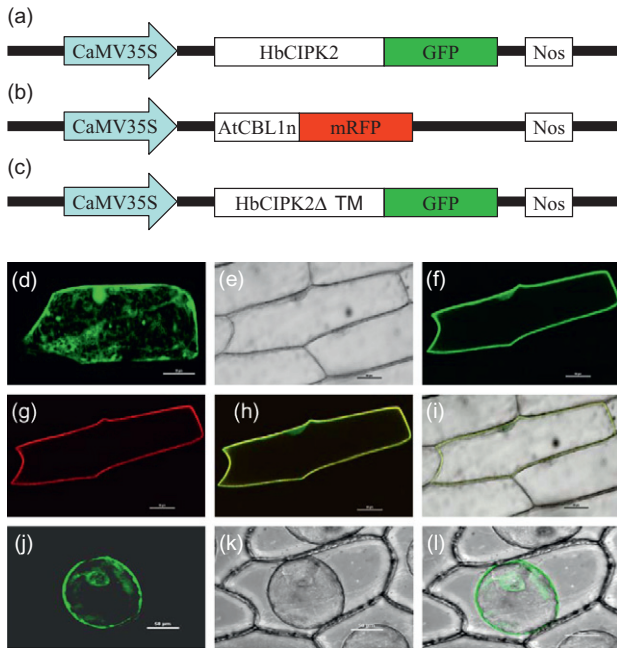


Figure 5. Subcellular localization of HbCIPK2-GFP fusion proteins in onion epidermal cells by particle bombardment. (a–c) The vectors were used for subcellular localization. (d) GFP fluorescence from epidermal cells bombarded with *p35S::GFP* as the control. (e–i) HbCIPK2-GFP and AtCBL1n-mRFP fusion proteins were transiently co-expressed into onion epidermal cells, and their localization was visualized by confocal microscopy 24 h post-transformation. AtCBL1n-mRFP was generated by using a primer binding to the mRFP 5' open reading frame (ORF) with an extension at the 5' end comprising the first 36 nucleotides of AtCBL1. (e) represents bright-field image of epidermal cells co-bombarded with *p35S::HbCIPK2-GFP* and *p35S::AtCBL1n-mRFP*. (f) represents the fluorescence associated with expression of HbCIPK2-GFP in the same cell. (g) represents the fluorescence associated with expression of a plasma membrane-localized maker, AtCBL1n-mRFP (Batistič *et al.* 2008, 2009). (h) shows an overlay between (f) and (g), and (i) is a merged image between (e) and (h). (j) represents the fluorescence associated with expression of HbCIPK2ΔTM-GFP only, visualizing under the treatment of 50% sucrose solution. (k) represents bright-field image of the same cell. (l) represents an overlay between (j) and (k). Bar = 50 μm.

generated by PCR amplification to fuse the first 12 amino acids of AtCBL1 (Batistič *et al.* 2008) to the N-terminus of mutated RFP (Fig. 5a–c). AtCBL1n-mRFP was used as a co-localization maker because AtCBL1n is localized to the plasma membrane but does not interact with CIPKs (Batistič *et al.* 2009). The two constructs were delivered into onion epidermal cells by particle co-bombardment, and transient expression of HbCIPK2-GFP was monitored by epi-fluorescence. The cell expressing GFP alone was detected with fluorescent signals in nucleus, membrane and cytoplasm as control (Fig. 5d). However, HbCIPK2-GFP was predominantly localized to the plasma membrane and nucleus while the AtCBL1n-mRFP was clearly targeted to the plasma membrane (Fig. 5e–i). Removal of a transmembrane helix domain located between amino acid residues

196 and 213 of HbCIPK2 resulted in non-specific expression pattern (Fig. 5j–l), similar to GFP alone. These results indicate that HbCIPK2 is mainly associated with the plasma membrane and nucleus, and that the specific structure and expression pattern are definitely involved with its function.

Overexpression of *HbCIPK2* rescued the salt hypersensitivity in *Arabidopsis* mutant *sos2-1*

To investigate whether *HbCIPK2* may rescue the salt-sensitive phenotype of *Arabidopsis* mutant *sos2-1*, *HbCIPK2* was overexpressed in *sos2-1* plants under the control of the CaMV 35S promoter. Over 10 independent transformed lines were generated, and the level of *HbCIPK2* transcript was evaluated by Northern blot analysis (Fig. 6e). Two homozygous lines (s6 and s11) were selected to test the response to salt stress.

To determine salt tolerance of the transgenic lines, the germination assay was first performed. At least 60 seeds of each transgenic line, WT and *sos2-1* were sown on MS plates with various concentration of NaCl. After germination for 7 d, the seeds that developed green cotyledons were scored. The transgenic lines showed significantly higher germination rates compared with the rates of the WT and *sos2-1* when sown with 125–150 mM NaCl; whereas under 100 mM NaCl stress, the germination rate of the two transgenic lines is significantly higher than the rate of *sos2-1*, but no difference from the WT; when seeds were sown without NaCl, all seeds of each transgenic line, WT or *sos2-1* almost had the germination rate of 100% (Fig. 6a).

Then seedling growth assay was used to further test the phenotype of the transgenic lines under salt stress. Growth of transgenic, WT and *sos2-1* seedlings on MS medium without salt was similar (Fig. 6c, left panel). However, when seedlings were transferred to medium with NaCl, the transgenic plants showed less growth inhibition in contrast to *sos2-1*, which almost became white and died (Fig. 6c, middle and right panels). It was obvious evidence that the average fresh weight of the transgenic lines was significantly higher than that of *sos2-1* and WT seedlings, especially at 150–175 mM NaCl (Fig. 6b).

To detect salt tolerance of plants when grown in soil, the WT, *sos2-1* and transgenic seeds were germinated in soil. Three-week-old plants were treated with NaCl by the addition of 50 mM increases every 2 d until a final concentration of 250 mM was reached. After stress of 1 week, the transgenic plants showed unaffected vegetative and reproductive growth in soil compared with growth of *sos2-1* plants, which lost vigour faster, and both vegetative and reproductive growth decreased, and last they became brown without any bolts. Although the WT plants exhibited normal vegetative growth, their bolts were fewer and shorter than that of the transgenic lines (Fig. 6d); no difference was found when plants were grown without NaCl (data not shown). All evidences above suggested that *HbCIPK2* may share common functions for ion homeostasis and salt tolerance with *Arabidopsis* AtCIPK24/SOS2, and that the expression of

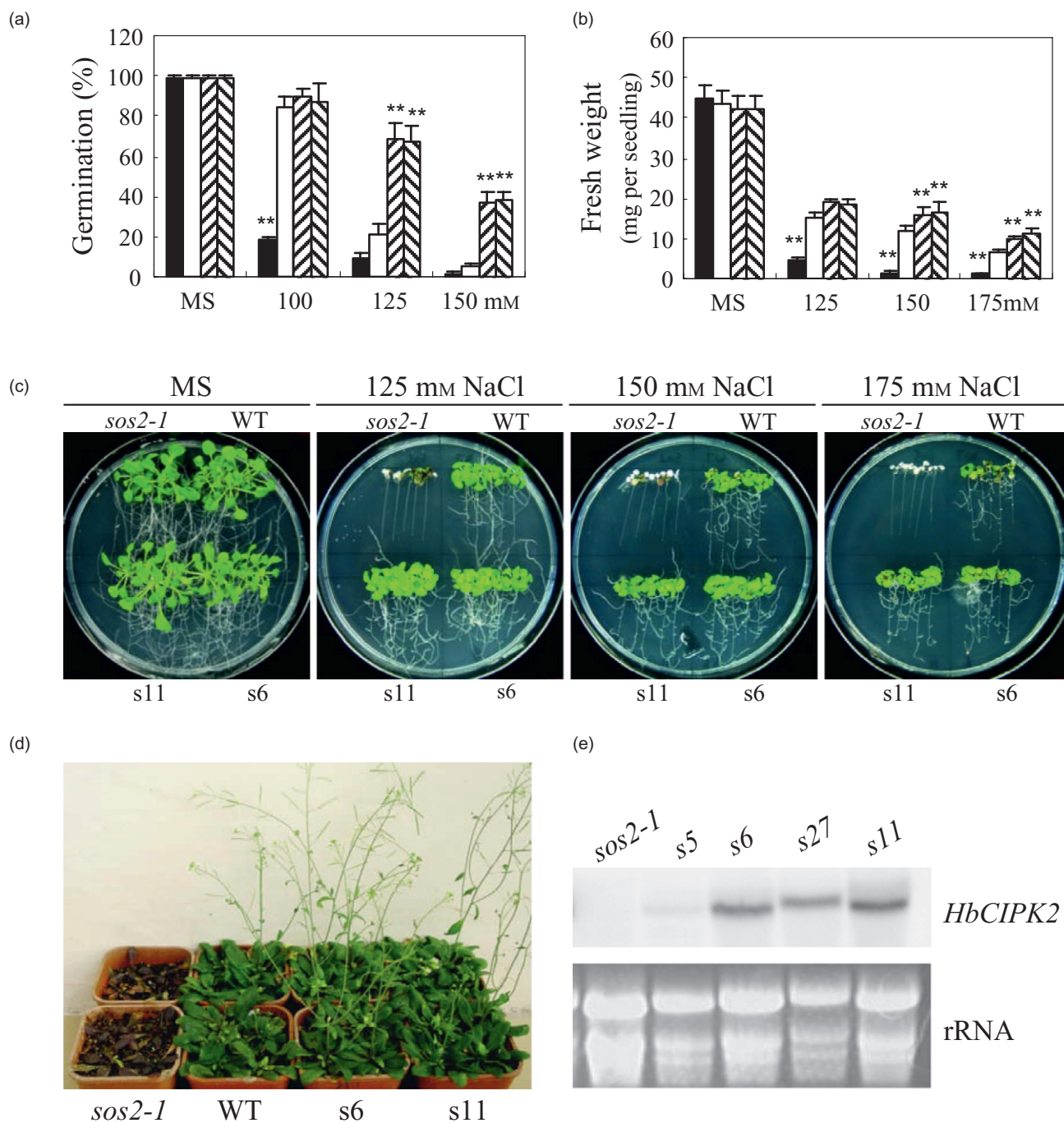


Figure 6. Overexpression of *HbCIPK2* rescued the salt hypersensitivity in *Arabidopsis sos2-1* mutant. *sos2-1*, *Arabidopsis sos2* mutant; WT, wild type; s5, 6, 11 and 27, four independent transgenic lines in *sos2-1* background, respectively. (a) Seed germination rates of *sos2-1*, WT, s6 and s11 on MS agar plates without or with different concentrations of NaCl. At least 60 seeds for each line with opening green cotyledons were scored at 7 d after transferring to 22 °C. (b) and (c) The seedling growth assays were performed. Fresh weight of seedling on vertical agar plates without or with different concentrations of NaCl was calculated, and at least 10 seedlings from each line were weighed after growing for 2 weeks (b). The photos were taken before weighing (c). (d) The phenotypes of 3-week-old plants subjected to salt stress with a final concentration of 250 mM NaCl by the addition of 50 mM increase every 2 d. The pictures show representative plants at 7 d post-treatment. (e) RNA gel blot analysis of *HbCIPK2* in *Arabidopsis sos2-1* mutant; ethidium bromide-stained rRNA bands were shown as a loading control. All assays were repeated three times, and all values are means of three replicates; the error bars indicated the standard deviation (SD). Asterisks above each column indicate a significant difference from WT at $P < 0.01$ level. Black, white, left-striped and right-striped columns represent *sos2-1*, WT, s6 and s11, respectively.

HbCIPK2 can rescue the salt hypersensitivity in *sos2-1* mutant, and specifically restore and promote the growth of shoots.

Overexpression of *HbCIPK2* in *Arabidopsis* WT enhanced salt tolerance

To analyse the function of *HbCIPK2* in details, the transgenic lines of *35S:HbCIPK2* in the *Arabidopsis* WT background were also generated and 28 independent homozygous T3 lines were produced. Under normal growth conditions, the transgenic lines exhibited no abnormal morphological phenotype compared with WT plants. Three of them were selected to evaluate the transcript level of *HbCIPK2* and their phenotype (Fig. 7e).

On MS plates with absence of NaCl, the phenotype of three transgenic lines was similar to that of WT plants; no difference was observed between them during germination, seedling growth and reproduction assays (Fig. 7a–c). However, seeds from the transgenic lines showed more rapid germination and higher rates than that of WT seeds on MS medium containing 125–150 mM NaCl (Fig. 7a). Growth of the transgenic seedlings was less inhibited compared with the WT seedlings under stress of 150–175 mM NaCl (Fig. 7c), which was confirmed by the average fresh weight of the WT and transgenic seedlings tested (Fig. 7b). The transgenic plants in soil under stress of 250 mM NaCl display improved growth with normal bolting, whereas the bolting was severely inhibited in the WT plants (Fig. 7d). All of these results indicate that *HbCIPK2* may function in salt tolerance pathway and the expression of *HbCIPK2* in *Arabidopsis* enhanced salt tolerance.

Overexpression of *HbCIPK2* increased osmotic stress tolerance

As *HbCIPK2* was also up-regulated by osmotic stress, we performed germination assay to assess tolerance to osmotic stress with five independent transgenic lines tested above. On MS medium containing no mannitol, the overexpressing *HbCIPK2* lines either in the WT or in mutant *sos2-1* background had no difference from the corresponding control (Fig. 8a,b). However, the germination rate of the WT seeds dramatically decreased on the medium containing high concentrations of mannitol (300–400 mM), but the *HbCIPK2*-overexpressing seeds still had higher germination rates compared with the WT (Fig. 8a). Interestingly, two transgenic lines (s6 and s11) showed similar germination percentage with *sos2-1*, which had higher germination rate than WT under stress of 300–400 mM mannitol. For example, on medium containing 350 mM mannitol, two transgenic lines overexpressing *HbCIPK2* showed 65 and 63% germination rates, and had no difference from *sos2-1* (60%), whereas WT seeds only had the rate of less than 20% (Fig. 8b). These results indicated that during seed germination, the role of *HbCIPK2* in response to osmotic

stress may be different from *AtCIPK24/SOS2*, at least to stress caused by mannitol.

Overexpression of *HbCIPK2* resulted in reduced Na⁺ and elevated K⁺ accumulation under salt stress

To find out the effect of overexpression of *HbCIPK2* on the accumulation of Na⁺ and K⁺, the content of these cations in roots and shoots of the control and transgenic lines was examined under normal condition and salt stress with ICP-AES. Under normal conditions, no difference was detected between the transgenic lines and the control either for Na⁺ or for K⁺ content. However, in short, under salt stress overexpression of *HbCIPK2* in the WT resulted in reduced Na⁺ accumulation only in shoot and elevated K⁺ content only in root (Fig. 9a,c), whereas in mutant *sos2-1* led to reduced Na⁺ and elevated K⁺ in both shoot and root (Fig. 9b,d).

Overexpression of *HbCIPK2* affected the flux of net H⁺ and K⁺ under salt stress

To determine the effect of overexpression of *HbCIPK2* on the ion fluxes, we used ~~SIET, namely microelectrode ion flux estimation (MIFE) assay~~, for H⁺ and K⁺ efflux measurements at the root apex. Five-day-old seedlings of WT, W116, *sos2-1* and s6 grown MS medium were transferred into Petri dish containing or without 75 mM NaCl for incubation of 30 min, then balanced in measuring buffer (0.1 mM KCl, 0.1 mM CaCl₂, 0.1 mM MgCl₂, 0.5 mM NaCl, 0.2 mM Na₂SO₄, 0.3 mM MES, pH 5.5) for 15 min. Net ion fluxes were measured from the root apex. For trans-membrane H⁺ flux, in normal condition it displayed influx for all seedlings of the transgenic and control lines, and no difference was detected between the transgenic and the control lines (data not shown). After NaCl stress, net H⁺ was changed to efflux, and the increases of H⁺ efflux in the transgenic line were more than that in the control (Fig. 9e,f). For K⁺ flux, it was different from H⁺ flux, and showed efflux for all seedlings for the transgenic and control lines under both normal condition (data not shown) and treatment of NaCl (Fig. 9g). Interestingly, K⁺ efflux decreased for all seedlings of the transgenic and control lines under salt stress compared with that in normal condition, but the transgenic seedlings showed less K⁺ efflux than control (Fig. 9g,h). It is likely that overexpression of *HbCIPK2* may result in higher H⁺ pump activity and prevention of K⁺ loss from root cells for maintaining cytosolic K⁺ homeostasis.

Overexpression of *HbCIPK2* protected root cell from death under salt stress

To investigate the effect of overexpression of *HbCIPK2* on salt-induced cell death and Na⁺ content *in vivo*, we used fluorescent dyes to stain the roots of 5-day-old transgenic and control seedlings grown on MS medium after 24 h of non-treatment or treatment of 125 mM NaCl, and observed

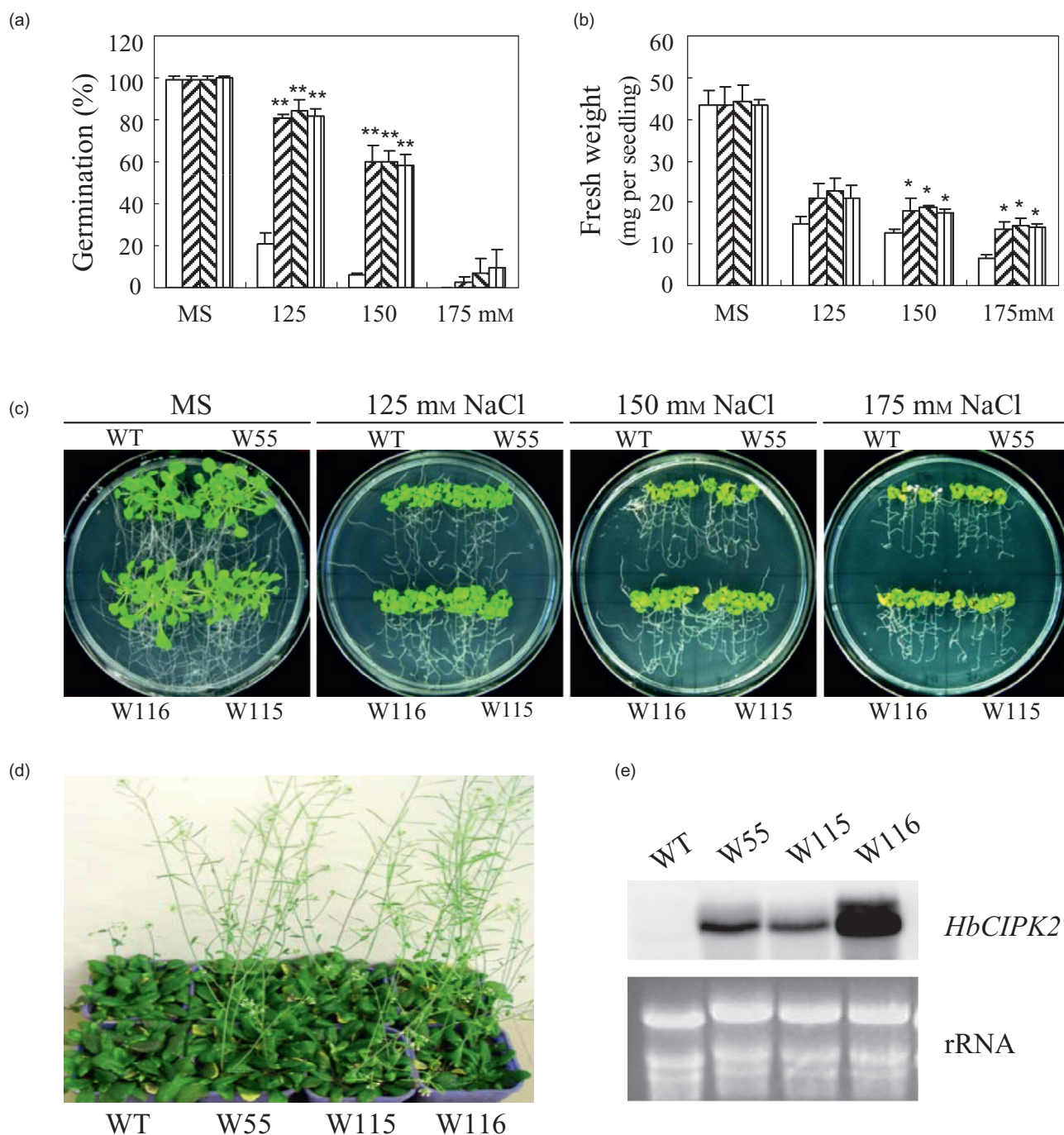


Figure 7. Overexpression of *HbCIPK2* enhanced the salt tolerance in *Arabidopsis* wild type. WT, wild type; W55, 115 and 116, three independent transgenic lines in WT background, respectively. (a) Seed germination rates of WT, W55, 115 and 116 on MS agar plates without or with different concentrations of NaCl. At least 60 seeds for each line with opening green cotyledons were scored at 7 d after transferring to 22 °C. (b) and (c) The seedling growth assays were performed. Fresh weight of seedling on vertical agar plates without or with different concentrations of NaCl. At least 10 seedlings from each line were weighed after growing for 2 weeks (b). The photos were taken before weighting (c). (d) The phenotypes of 3-week-old plants subjected to salt stress with a final concentration of 250 mM NaCl by the addition of 50 mM increases every 2 d. The pictures show representative plants at 7 d post-treatment. (e) RNA gel blot analysis of *HbCIPK2* in *Arabidopsis* WT; ethidium bromide-stained rRNA bands were shown as a loading control. All assays were repeated three times, and all values are means of three replicates; the error bars indicated the standard deviation (SD). Asterisks (**) above each column indicate a significant difference from WT at $P < 0.01$ level. Asterisk (*) indicates a difference at $P < 0.05$ level. White, left-striped, right-striped and straight-striped columns represent WT, W55, 115 and 116, respectively.

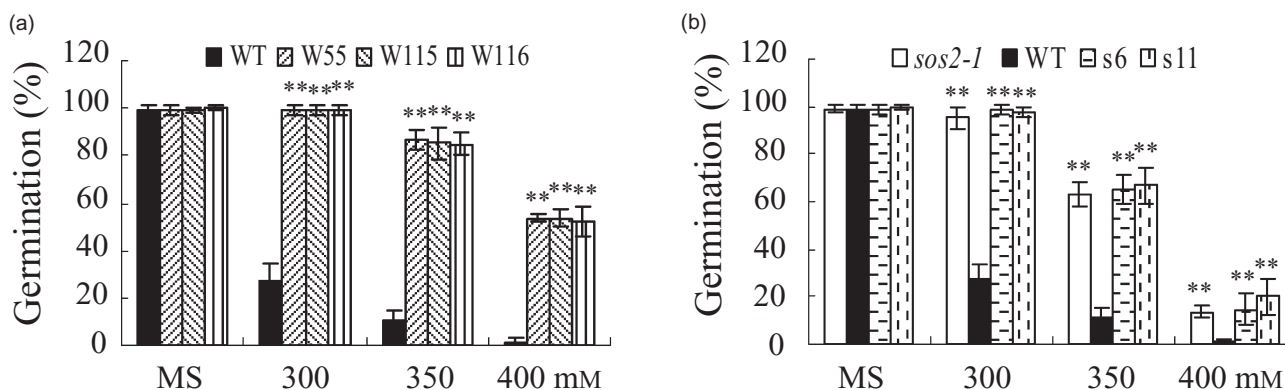


Figure 8. *HbCIPK2*-overexpressing *Arabidopsis* plants enhanced osmotic stress. (a) and (b) seed germination rates of WT, *sos2-1* and transgenic lines on MS agar plates without or with different concentration of mannitol. At least 60 seeds for each line were sown on the indicated medium; germinated seeds with opening green cotyledons were scored at 7 d after transferring to 22 °C. All values are means \pm SD ($n = 3$); SD was shown as standard error for at least three replicates. Asterisks above each column indicate a significant difference from WT at $P < 0.01$ level.

fluorescent signals by confocal microscopy. A sodium-specific fluorescent dye, CoroNa-Green (Invitrogen), was used to visualize Na^+ *in vivo*, and propidium iodide (Invitrogen) was indicator for dead cells. Under normal condition, no significant differences in fluorescence intensity imaging neither for Na^+ nor for dead cells were observed between cells of transgenic seedlings and control in the root meristem in spite of the presence of background fluorescence (data not shown). By contrast, for Na^+ -imaged fluorescence, differences appeared in the root tips of *Arabidopsis sos2-1* mutant and the transgenic line s6 under salt stress (Fig. 10), while no differences were detected between WT and the transgenic line W116, which is consistent with the results of Na^+ content measured. Interestingly, propidium iodide fluorescences in the transgenic roots were significantly weaker than that in roots of control seedlings, and salt-induced dead cells of the transgenic root dyed in red were less than that of control. This result indicated that overexpression of *HbCIPK2* protected root cell from death under salt stress, which is consistent with imaging of Na^+ content *in vivo*.

Overexpression of *HbCIPK2* caused coordinated changes in gene expression under salt stress

To analyse the transcript changes of downstream genes affected by overexpression of *HbCIPK2*, Agilent *Arabidopsis* microarrays were used to compare genome-wide transcripts from 10-day-old seedlings of WT with that from one *HbCIPK2*-overexpressing line (W116). To assess the reproducibility of microarray signals, we performed three biological replicates for both WT and W116. Thinking of the transgenic lines exhibiting salt tolerance in saline condition, we carried out the chip assays with seedlings grown in non-saline and saline conditions, respectively. Under normal condition, only a total of 46 genes were found to show at

least twofold expression changes between transgenic line and WT at $P < 0.05$, and most of which had no obvious function annotation with low log₂-fold changes ranging from 2.0 to 1.0 (Supporting Information Table S2). Under salt stress of 150 mM NaCl for 12 h, a total of 200 differentially expressed genes excluding the effects of growth conditions and sampling were identified between 35S:*HbCIPK2* line and WT, among which 140 (70%) were up-regulated and 60 (30%) were down-regulated with fold changes higher than 2 (Supporting Information Table S3). Among differentially expressed genes, about 20% were unknown genes; over 25% were involved in responses to stress; others were related to metabolism, protein fate, transcription regulation and signal transduction, implying that *HbCIPK2* may be involved in multiple processes of expression regulation. Up-regulated genes responsive to stress in *HbCIPK2*-overexpressing line were represented in Table 1. These genes with altered expression levels were functionally grouped into five categories: (1) response to abiotic stress (e.g. *CYP705A32* and *ATPER1*); (2) response to biotic stimuli (e.g. *PRI* and *ARD*); (3) ion transport or binding (e.g. *HAK*); (4) signalling system (e.g. *CaBP*, Calcium-binding EF hand family protein); (5) transcription regulation (e.g. *WRKY* and *AP2-TF*). Seven genes encoding protein kinases and three genes encoding Ca^{2+} sensor or receptors were up-regulated in *HbCIPK2*-overexpressing line, suggesting that *HbCIPK2*, a novel member of serine/threonine protein kinase, may promote expression changes of other kinases or be involved in complex interaction/phosphorylation in response to salt stress. *ARD* (AT2G26400) may be involved in ethylene signalling in response to biotic and abiotic stress (Xu *et al.* 2010). *CYP76C6* (AT1G33720) and *CYP705A5* (AT5G47990) were responsible for oxygen binding that scavenges ROS and maintains ROS homeostasis. *ATPER1* (AT1G48130) were responsive to oxidative stress (Haslekäs *et al.* 2003). Interestingly, several genes related to pathogen or disease

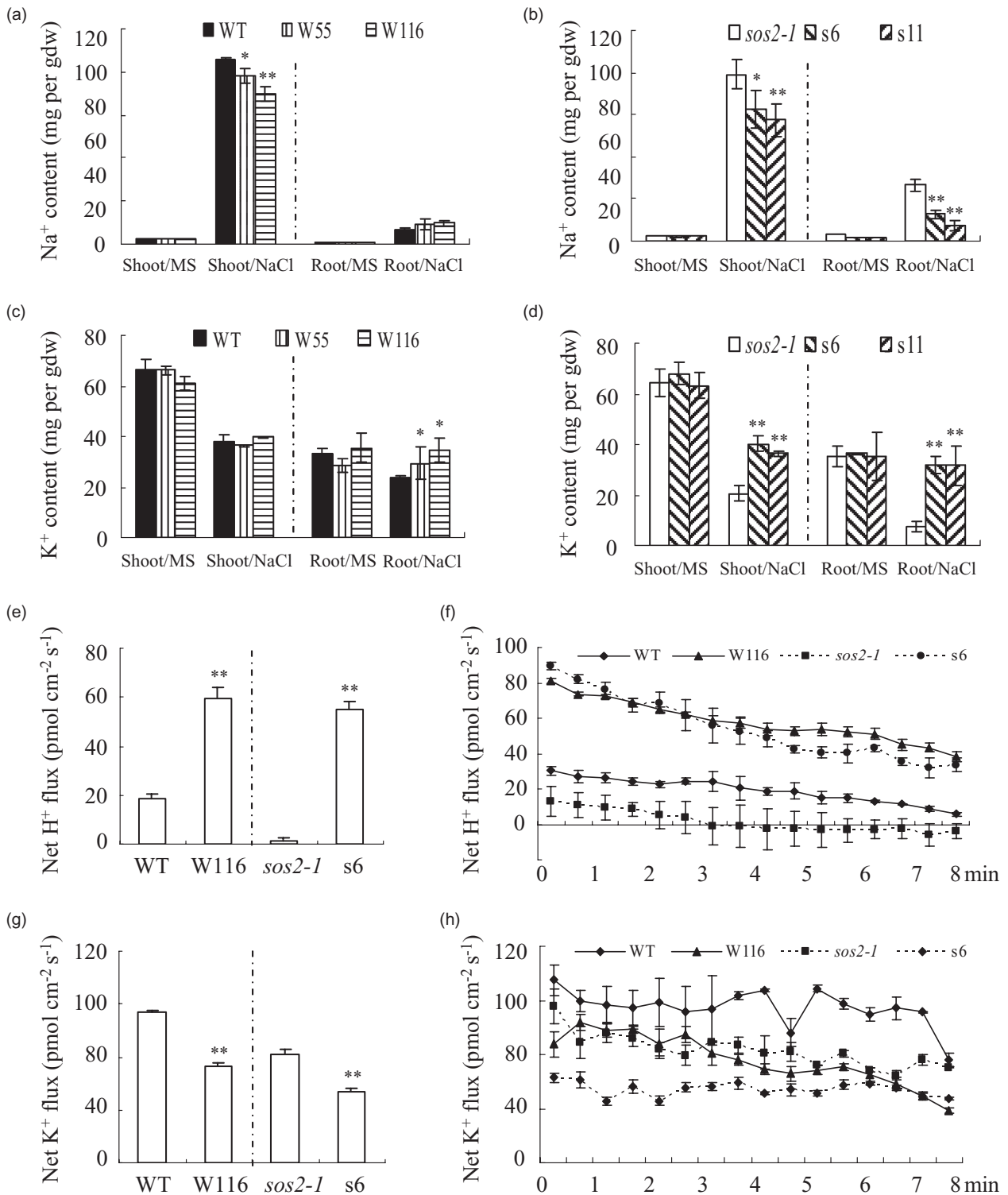


Figure 9. Overexpression of *HbCIPK2* affected the flux of net H⁺ and K⁺ under salt stress. (a) and (b) Na⁺ contents; (c) and (d) K⁺ contents in roots and shoots of 10-day-old seedlings of the transgenic lines and the control on MS agar plates with 100 mM NaCl for 10 d. (e) to (h) The net H⁺ and K⁺ effluxes in roots of WT, W116, *sos2-1* and *s6* plants. The SIET technique was used for non-invasive ion flux measurement. (e) Means of the net proton effluxes calculated from (f) within 8 min of the measurement time. (f) Dynamic changes of the net proton effluxes in the transgenic lines and the control root tips within 8 min. (g) Means of net K⁺ effluxes calculated from (h) within 8 min of the measurement time. (h) Dynamic changes of the net K⁺ effluxes in the transgenic lines and the control root tips within 8 min. After roots were treated with 75 mM NaCl for 30 min, transient net H⁺ and K⁺ flux were recorded, respectively. All assays were repeated three times, and all values are means of three replicates; the error bars indicated the standard deviation (SD). Asterisks (**) above each column indicate a significant difference from WT or *sos2-1* at $P < 0.01$ level. Asterisk (*) indicates a difference at $P < 0.05$ level.

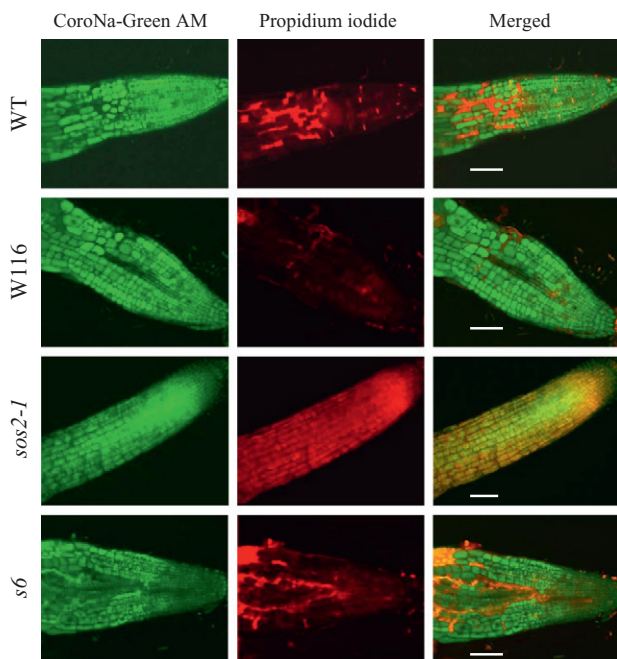


Figure 10. Na^+ and dead cells in the roots of wild type (WT), *sos2-1* and transgenic seedlings were imaged under salt stress. Roots of 5-day-old WT (first line), W116 (second line), *sos2-1* (third line) and *s6* (last line) seedlings were stained with CoroNa-Green AM after 24 h of 125 mM NaCl treatment and observed with a confocal microscope (first column). Propidium iodide ($1 \mu\text{g mL}^{-1}$) was added to stain the damaged cells in the second column. All merged images are shown in the last column. Bars = $10 \mu\text{m}$.

resistance were up-regulated. However, among down-regulated genes, about 33% were unknown genes, 20% were gene family member encoding heat shock protein and others were involved in diverse biological processes. The results of microarray analyses revealed that *HbCIPK2* regulated target genes only under stress, not constitutively, and overexpression of *HbCIPK2* caused coordinated changes in gene expression under stress.

To verify the microarray data, qRT-PCR was carried out with W116, *s6* and the corresponding control under salt stress, and 12 differentially expressed genes were focused on. Genes subjected to validation were *PCC1* (AT3G22231), *PK* (AT5G38250), *HMADP* (AT5G26690), *ANK* (AT5G54610), *ZIB* (AT1G05880), *AP2-TF* (AT1G19210), *WRKY62* (AT5G01900), *ATPase* (AT3G28510), *CaBP* (AT3G47480), *CYP705A5* (AT5G47990), *HAK5* (AT4G13420) and *AtTIP2;3* (AT5G47450). The expression change levels of tested genes by qRT-PCR were closely correlated with changes detected through microarray analysis when transcripts in W116 were compared with that in WT, confirming the reliability of the microarray results (Fig. 11, Table 1). Surprisingly, *HAK5* was up-regulated in two transgenic lines, just significantly in *s6*. These results indicated that overexpression of *HbCIPK2* in different backgrounds may result in coordinated expression changes of different genes.

DISCUSSION

The importance of identification of a CIPK protein from halophytic grass

Due to natural selection and adaptation to stressful environment, halophytes may evolve the specific or diverse regulatory mechanisms to tolerate high salinity. Moreover, there is significant plasticity in environmental adaptation for halophyte. Thus, the basic machinery for adaptation to high salinity deserves research. However, because of the difference in the use of Na^+ and K^+ between mono- and dicotyledonous halophytes and the great importance of cereals as crop means, it seems more important to dissect the regulatory mechanisms for salt tolerance in monocotyledonous halophytes (Flowers & Colmer 2008). To date, although there is evidence that the high selectivity for K^+ over Na^+ contributes salt tolerance in halophytic grass, in general which proteins and regulatory networks are involved remain unknown (Wang *et al.* 2009).

In this paper, we address these goals by identifying differentially expressed genes from a halophytic grass. Our strategy was to employ *H. brevisubulatum* to screen differentially expressed genes by cDNA-AFLP technique under salt stress. Due to the importance of CIPK proteins in abiotic stress response and transducer in stress signalling networks in glycophytes, we have concentrated on a CIPK protein from *H. brevisubulatum*, named as HbCIPK2. Comparison of HbCIPK2 with CIPKs in glycophytes revealed similarities in the synteny and protein structure. However, there are some differences in expression patterns and functional characteristics between HbCIPK2 and CIPKs from glycophytes. Some of these may be expected to be related to different salt signalling pathway or salt tolerance in halophyte.

Differences between HbCIPK2 and AtCIPK2 or AtCIPK24

Based on blast search of HbCIPK2, as for typical glycophytes such as *Arabidopsis* and rice, AtCIPK2 and OsCIPK2 were its orthologs among 26 CIPKs in *Arabidopsis* and 30 members in rice, respectively (Fig. 2a). However, few reports focused on their roles in salt tolerance. Here we report that HbCIPK2, a novel member of CIPK family, is a positive regulator of salt tolerance from halophytic grass. If it is confirmed that AtCIPK2 or OsCIPK2 is not associated with salt tolerance, it is unclear whether the differences in conferring salt tolerance between HbCIPK2 and AtCIPK2 or OsCIPK2 result from evolutionary divergence between halophyte and glycophyte.

AtCIPK24/SOS2 is one of the best-characterized components in the salt stress signalling, and is required for salt tolerance (Liu *et al.* 2000; Guo *et al.* 2001, 2004). Moreover, the SOS pathway is conserved in rice (Martínez-Atienza *et al.* 2007). HbCIPK2, a SOS2-like protein, has been identified from *H. brevisubulatum*. The differences between HbCIPK2 and AtCIPK24 involve multiple aspects including phylogenetic relationship, structure

Table 1. Gene products of selected up-regulated transcripts ($P < 0.05$) in *HbCIPK2*-overexpressing line W116 compared with wild-type (WT) plants

Accession	Gene product	Gene ontology	Log2 fold
AT2G14610	PR1	Defence response	5.9
AT3G22231*	PCC1	Response to biotic stress	5.9
AT2G24850	TAT3 (Tyrosine aminotransferase 3)	Response to jasmonic acid stimulus	3.7
AT5G38250*	Serine/threonine protein kinase	Phosphorylation	3.3
AT5G26690*	Heavy-metal-associated domain-containing protein	Cation transport	3.2
AT5G54610*	ANK (ANKYRIN)	Response to salicylic acid stimulus	3.1
AT4G04500	Protein kinase family protein	Phosphorylation	3.0
AT1G05880*	Zinc ion binding	Ion binding	2.6
AT4G03450	Ankyrin repeat family protein	Protein binding	2.5
AT5G52760	Heavy-metal-associated domain-containing protein	Metal ion transport	2.5
AT2G26400	ARD/ATARD3 (Acireductone dioxygenase)	Response to stress	2.3
AT1G19210*	AP2 domain-containing transcription factor	Response to ethylene stimulus	2.2
AT5G01900*	WRKY62 (WRKY DNA-binding protein 62)	Regulation of transcription	2.1
AT1G35710	Leucine-rich repeat transmembrane protein kinase	Phosphorylation	2.1
AT4G23310	Receptor-like protein kinase	Defence response	2.1
AT3G25010	Disease resistance family protein	Defence response	2.0
AT3G28510*	AAA-type ATPase family protein	ATPase activity	2.0
AT3G23120	Leucine-rich repeat family protein	Defence response	2.0
AT5G55460	Protease inhibitor	Defence response	2.0
AT4G23200	Protein kinase family protein	Phosphorylation	2.0
AT4G05030	Heavy-metal-associated domain-containing protein	Metal ion transport	2.0
AT4G11170	Disease resistance protein (TIR-NBS-LRR class)	Defence response	1.9
AT3G20950	CYP705A32	Response to abiotic stimulus	1.9
AT1G65790	ARK1 (<i>A. thaliana</i> receptor kinase 1)	Phosphorylation	1.8
AT4G34410	AP2 domain-containing transcription factor	Regulation of transcription	1.8
AT1G71390	Disease resistance family protein	Defence response	1.7
AT4G04510	Protein kinase family protein	Phosphorylation	1.7
AT1G21240	WAK3 (Wall-associated kinase 3)	Phosphorylation	1.7
AT1G73805	Calmodulin binding	Ca ²⁺ sensor	1.6
AT5G26170	WRKY50 (WRKY DNA-binding protein 50)	Regulation of transcription	1.6
AT5G21960	AP2 domain-containing transcription factor	Regulation of transcription	1.6
AT3G47480*	Calcium-binding EF hand family protein	Calcium ion binding	1.5
AT2G46400	WRKY46 (WRKY DNA-binding protein 46)	Regulation of transcription	1.5
AT5G52720	Metal ion binding	Metal ion transport	1.5
AT3G56400	WRKY70 (WRKY DNA-binding protein 70)	Regulation of defence response	1.5
AT1G72910	Disease resistance protein (TIR-NBS class)	Defence response	1.5
AT3G46090	ZAT7	Response to stress	1.4
AT3G28540	AAA-type ATPase family protein	ATP binding	1.4
AT5G39670	Calcium-binding EF hand family protein	Calcium ion binding	1.4
AT5G60900	RLK1 (Receptor-Like protein kinase 1)	Phosphorylation	1.4
AT2G22760	Basic helix-loop-helix (bHLH) family protein	Regulation of transcription	1.4
AT5G22380	ANAC090	Regulation of transcription	1.4
AT5G66890	Disease resistance protein (CC-NBS-LRR class)	Defence response	1.3
AT3G22910	Calcium-transporting ATPase	Cation transport	1.3
AT1G33720	CYP76C6	Oxygen binding	1.2
AT1G74930	ORA47	Response to ethylene stimulus	1.2
AT2G44840	ATERF13/EREBP	Response to ethylene stimulus	1.2
AT5G47990*	CYP705A5	Oxygen binding	1.1
AT1G48130	ATPER1	Response to water deprivation	1.1
AT4G25490	CBF1	Response to water deprivation	1.1
AT2G41090	Calmodulin-like calcium-binding protein	Phosphatidylinositol signalling	1.0
AT4G13420*	HAK5 (High affinity K ⁺ transporter 5)	Potassium ion transport	0.6
AT5G47450*	AtTIP2;3	Water transport	0.2

Log2 fold indicates the average up-regulation of line W116 compared with WT in three biological replicates. Genes marked with asterisks were selected to further verify their expression between transgenic line and control plants under salt stress via real-time PCR.

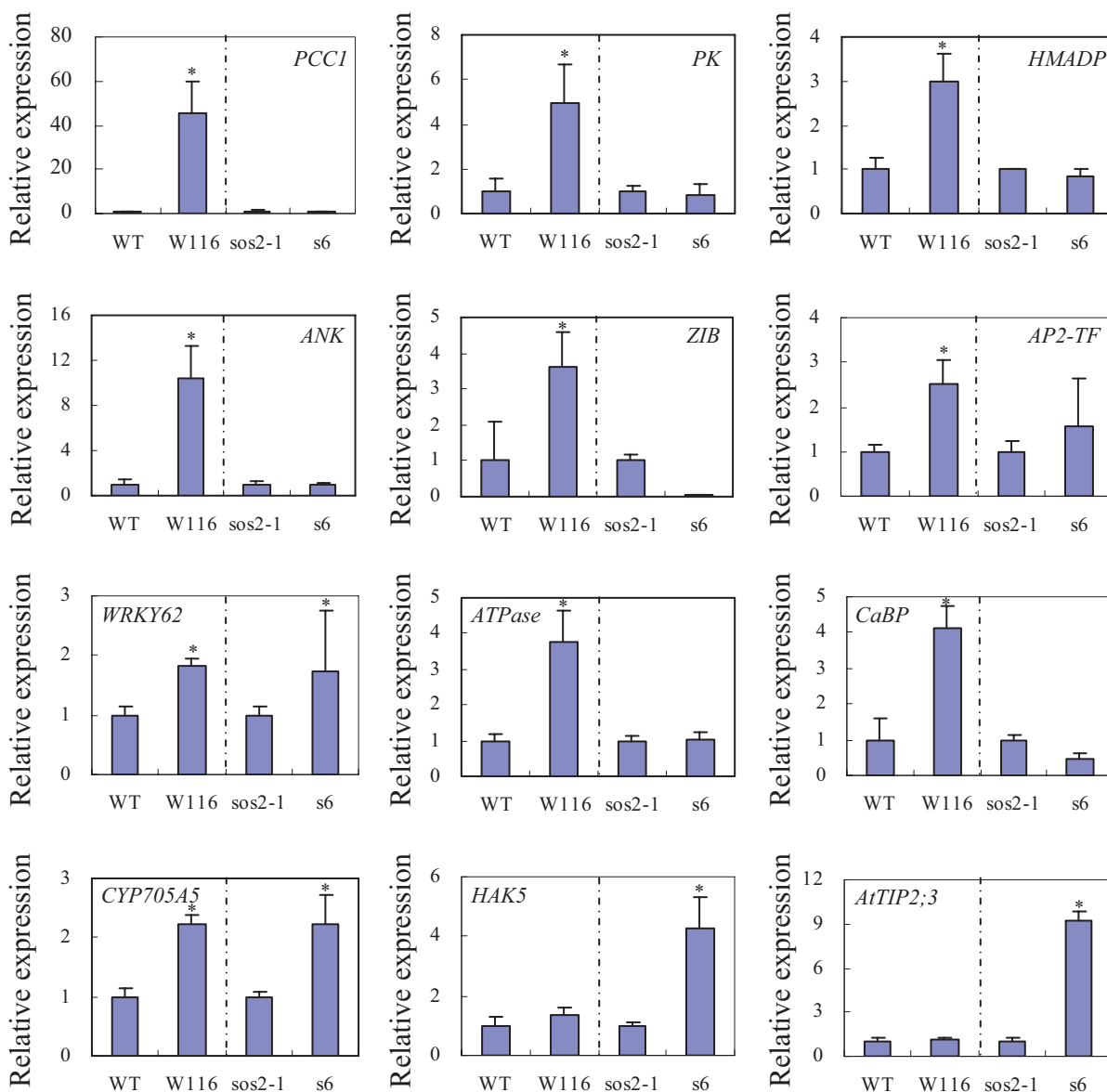


Figure 11. The transcripts of candidate target genes are regulated by overexpression of *HbCIPK2* in *Arabidopsis*. The selected genes included: *PCC1* (AT3G22231), *PK* (AT5G38250, serine/threonine protein kinase), *HMADP* (AT5G26690, heavy-metal-associated domain-containing protein), *ANK* (AT5G54610), *ZIB* (AT1G05880, zinc ion binding), *AP2-TF* (AT1G19210), *WRKY62* (AT5G01900), *ATPase* (AT3G28510), *CaBP* (AT3G47480, calcium-binding EF hand family protein), *CYP705A5* (AT5G47990), *HAK5* (AT4G13420), *AtTIP2;3* (AT5G47450). Total RNA was isolated from 10-day-old seedlings grown on vertical MS plates after treatment of 150 mM NaCl and used for qRT-PCR. Bars indicate mean relative expression values \pm standard error. *18S rRNA* was used as a housekeeping gene. Asterisks indicate significant differences between transgenic and control plants ($P < 0.05$).

character, expression pattern, subcellular localization, and regulation of ionic and osmotic homeostasis. *AtCIPK24* belongs to intron-harboring subgroup with 12 introns (Kolukisaoglu *et al.* 2004), it mainly distributes cytoplasm due to no specific domain such as transmembrane motif (Quan *et al.* 2007), and its transcript is up-regulated only in root and not in shoot under salt stress (Liu *et al.* 2000). In contrast, here *HbCIPK2* has no intron, belonging to intron-less subgroup of *CIPK* gene family, and is localized at the plasma membrane and nucleus in cells due to the transmembrane helix domain located between amino acid

residues 196 and 213. *HbCIPK2* is strongly induced not only in root but also in shoot by high salinity, drought and ABA treatment (data not shown). Recently, it has been shown that stress-independent gene expression strength or transcript stability may be a crucial characteristic that distinguishes halophytes from glycophytes (Dassanayake *et al.* 2011). Although comparison of *HbCIPK2* transcript with that of *AtCIPK2* did not perform in the same experiences, it is evidence that *HbCIPK2* was identified by cDNA-AFLP technique due to its significantly differential expression.

Remarkably, HbCIPK2 may function in different ways from AtCIPK24. According to the report by Guo *et al.* (2004), it is shown that overexpression of *AtCIPK24/SOS2* in *sos2* background only could rescue the hypersensitivity of *sos2*, whereas overexpression of *HbCIPK2* in *sos2* background not only did but also beyond that of WT plant; overexpression of HbCIPK2 in *Arabidopsis* WT could improve salt tolerance just as ectopic expression of the activated forms T/DSOS2 and T/DSOS2/DF did. To some extent, it is possible that HbCIPK2 identified from halophyte has more kinase activities than AtCIPK24 from glycophyte as expected. However, whether the properties of HbCIPK2 are derived from selection and adaptation during a long time is unknown. In addition, K⁺ homeostasis is of critical importance in salt tolerance in higher plants. There are evidences that some K⁺ transporters or channels participate to retain K⁺ homeostasis (Rus *et al.* 2004; Xu *et al.* 2006; Nieves-Cordones *et al.* 2010). However, whether AtCIPK24 targets a K⁺ transporter is still unknown. Interestingly, based on the phenotypes and the data of ion contents and fluxes of *HbCIPK2*-overexpressing lines under salt stress, it implies that HbCIPK2 confers salt tolerance through not only regulating Na⁺ transporter activity but also mediating activity of K⁺ transporter, just as supported by the interaction of HbCIPK2 with a Na⁺-H⁺ transporter and a K⁺ transporter, respectively (unpublished data). These findings imply novel salt signalling pathways or networks by HbCIPK2 mediation.

Another difference between HbCIPK2 and AtCIPK24 might be the regulation of osmotic homeostasis. Several osmotic stress-activated CIPKs probably mediate osmotic stress signalling, but not AtCIPK24 (Zhu 2002). Our results showed overexpression of *HbCIPK2* in *Arabidopsis* WT also increased osmotic stress tolerance during seed germination, but *sos2-1* displayed higher germination rate, implying that HbCIPK2 may be a positive regulator in osmotic stress response, whereas SOS2 might not at least. It can explain that expression changes of selected genes by qRT-PCR in WT background are not similar to that in *sos2-1* background.

As salt-triggered signal transducers, the differences in function between HbCIPK2 and AtCIPK24 may involve different salt signalling pathways or networks, which may be one of important contributors to salt tolerance in *H. brevisubulatum*. With the advent of ongoing barley genome sequences release and comparisons of halophyte transcriptomes to glycophytic relatives, novel salt signalling pathways mediated by HbCIPK2 and more will be elucidated, and the essence of halophytism in *H. brevisubulatum* may be explained.

In conclusion, we identified a novel CIPK protein from halophyte and found that the expression of *HbCIPK2* is strongly induced by salinity, drought and ABA. Overexpression of *HbCIPK2* in *Arabidopsis* could enhance salt tolerance by the ability of maintaining K⁺/Na⁺ homeostasis and protection of root cell from death under salt stress. HbCIPK2-mediated K⁺ homeostasis may be a new insight

in salt response, which could be different from the SOS pathway. Our work established a new mechanism for HbCIPK2 in conferring salt tolerance.

ACKNOWLEDGMENTS

We thank Dr. Xin Deng (Institute of Botany, Chinese Academy of Sciences) for the plasmid containing *mRFP* gene. We are grateful to the National Transgenic Major Program of China (2009ZX08009-060B), the National Natural Science Foundation of China (30971850), Beijing Natural Science Foundation (5102017) and the General Program of Beijing Academy of Agriculture and Forestry Sciences (2010A003) for the financial support.

REFERENCES

- Apse M.P., Sottosanto J.B. & Blumwald E. (2003) Vacuolar cation/H⁺ exchange, ion homeostasis, and leaf development are altered in a T-DNA insertional mutant of AtNHX1, the *Arabidopsis* vacuolar Na⁺/H⁺ antiporter. *The Plant Journal* **36**, 229–239.
- Bachem C.W.B., Oomen R.J.F.J. & Visser R.G.F. (1998) Transcript imaging with cDNA-AFLP: a step-by-step protocol. *Plant Molecular Biology Reporter* **16**, 157–173.
- Batistić O., Sorek N., Schültke S., Yalovsky S. & Kudla J. (2008) Dual fatty acyl modification determines the localization and plasma membrane targeting of CBL/CIPK Ca²⁺ signaling complexes in *Arabidopsis*. *The Plant Cell* **20**, 1346–1362.
- Batistić O., Waadt R., Steinhorst L., Held K. & Kudla J. (2009) CBL-mediated targeting of CIPKs facilitates the decoding of calcium signals emanating from distinct cellular stores. *The Plant Journal* **61**, 211–222.
- Clough S.J. & Bent A.F. (1998) Floral dip: a simplified method for *Agrobacterium*-mediated transformation of *Arabidopsis thaliana*. *The Plant Journal* **16**, 735–743.
- Das R. & Pandey G.K. (2010) Expressional analysis and role of calcium regulated kinases in abiotic stress signaling. *Current Genomics* **11**, 2–13.
- Dassanayake M., Oh D.H., Hong H., Bohnert H.J. & Cheeseman J.M. (2011) Transcription strength and halophytic lifestyle. *Trends in Plant Science* **16**, 1–3.
- Du W., Lin H., Chen S., Wu Y., Zhang J., Fuglsang A.T., Palmgren M.G., Wu W. & Guo Y. (2011) Phosphorylation of SOS3-like calcium-binding proteins by their interacting SOS2-like protein kinases is a common regulatory mechanism in *Arabidopsis*. *Plant Physiology* **156**, 2235–2243.
- Flowers T.J. (2004) Improving crop salt tolerance. *Journal of Experimental Botany* **55**, 307–319.
- Flowers T.J. & Colmer T.D. (2008) Salinity tolerance in halophytes. *New Phytologist* **179**, 945–963.
- Fuglsang A.T., Guo Y., Cui T.A., *et al.* (2007) *Arabidopsis* protein kinase PKS5 inhibits the plasma membrane H⁺-ATPase by preventing interaction with 14-3-3 protein. *The Plant Cell* **19**, 1617–1634.
- Fujii H., Verslues P.E. & Zhu J.-K. (2011) *Arabidopsis* decuple mutant reveals the importance of SnRK2 kinases in osmotic stress responses in vivo. *Proceedings of the National Academy of Sciences of the United States of America* **97**, 1717–1722.
- Guo Y., Halfter U., Ishitani M. & Zhu J.K. (2001) Molecular characterization of functional domains in the protein kinase SOS2 that is required for plant salt tolerance. *The Plant Cell* **13**, 1383–1399.

- Guo Y., Qiu Q.S., Quintero F.J., Pardo J.M., Ohta M., Zhang C.Q., Schumaker K.S. & Zhu J.K. (2004) Transgenic evaluation of activated mutant alleles of SOS2 reveals a critical requirement for its kinase activity and C-terminal regulatory domain for salt tolerance in *Arabidopsis thaliana*. *The Plant Cell* **16**, 435–449.
- Hall D., Evans A.R., Newbury H.J. & Pritchard J. (2006) Functional analysis of CHX21: a putative sodium transporter in *Arabidopsis*. *Journal of Experimental Botany* **57**, 1201–1210.
- Hasegawa P.M., Bressan R.A., Zhu J.K. & Bohnert H.J. (2000) Plant cellular and molecular responses to high salinity. *Annual Review of Plant Physiology and Plant Molecular Biology* **51**, 463–499.
- Haslekás C., Grini P.E., Nordgard S.H., Thorstensen T., Viken M., Nygaard V. & Aalen R.B. (2003) ABI3 mediates expression of the peroxiredoxin antioxidant *AtPER1* gene and induction by oxidative stress. *Plant Molecular Biology* **53**, 313–326.
- Hauser F. & Horie T. (2010) A conserved primary salt tolerance mechanism mediated by HKT transporters: a mechanism for sodium exclusion and maintenance of high K⁺/Na⁺ ratio in leaves during salinity stress. *Plant, Cell & Environment* **33**, 552–565.
- Hellens R.P., Edwards E.A., Leyland N.R., Bean S. & Mullineaux P.M. (2000) pGreen: a versatile and flexible binary Ti vector for *Agrobacterium*-mediated plant transformation. *Plant Molecular Biology* **42**, 819–832.
- Huang C., Ding S., Zhang H., Du H. & An L. (2011) CIPK7 is involved in cold response by interacting with CBL1 in *Arabidopsis thaliana*. *Plant Science* **18**, 57–64.
- Katiyar-Agarwal S., Zhu J., Kim K., Agarwal M., Fu X., Huang A. & Zhu J.K. (2006) The plasma membrane Na⁺/H⁺ antiporter SOS1 interacts with RCD1 and functions in oxidative stress tolerance in *Arabidopsis*. *Proceedings of the National Academy of Sciences of the United States of America* **103**, 18816–18821.
- Kim S., Kang J.Y., Cho D.I., Park J.H. & Kim S.Y. (2004) ABF2, an ABRE-binding bZIP factor, is an essential component of glucose signaling and its overexpression affects multiple stress tolerance. *The Plant Journal* **40**, 75–87.
- Kolkisaoglu U., Weinel S., Blazevic D., Batistič O. & Kudla J. (2004) Calcium sensors and their interacting protein kinases: genomics of the *Arabidopsis* and rice CBL-CIPK signaling networks. *Plant Physiology* **134**, 43–58.
- Komatsuda T., Tanno K., Salomon B., Bryngelsson T. & Bothmer R. (1999) Phylogeny in the genus *Hordeum* based on nucleotide sequences closely linked to the *vrs1* locus (row number of spikelets). *Genome* **42**, 973–981.
- Kudla J., Batistič O. & Hashimoto K. (2010) Calcium signals: the lead currency of plant information processing. *The Plant Cell* **22**, 541–563.
- Lee S.C., Lan W.Z., Kim B.G., Li L., Cheong Y.H., Pandey G.K., Lu G., Buchanan B.B. & Luan S. (2007) A protein phosphorylation/dephosphorylation network regulates a plant potassium channel. *Proceedings of the National Academy of Sciences of the United States of America* **104**, 15959–15964.
- Li R., Zhang J., Wei J., Wang H., Wang Y. & Ma R. (2009) Functions and mechanisms of the CBL-CIPK signaling system in plant response to abiotic stress. *Progress in Natural Science* **19**, 667–676.
- Lin H., Yang Y., Quan R., Mendoza I., Wu Y., Du W., Zhao S., Schumaker K.S., Pardo J.M. & Guo Y. (2009) Phosphorylation of SOS3-LIKE CALCIUM BINDING PROTEIN8 by SOS2 protein kinase stabilizes their protein complex and regulates salt tolerance in *Arabidopsis*. *The Plant Cell* **21**, 1607–1619.
- Liu J., Ishitani M., Halfter U., Kim C.S. & Zhu J.K. (2000) The *Arabidopsis thaliana* SOS2 gene encodes a protein kinase that is required for salt tolerance. *Proceedings of the National Academy of Sciences of the United States of America* **97**, 3730–3734.
- Livak K.J. & Schmittgen T.D. (2001) Analysis of relative gene expression data using real-time quantitative PCR and the 2^{-ΔΔC_t} method. *Methods* **25**, 402–408.
- Luan S. (2009) The CBL-CIPK network in plant calcium signaling. *Trends in Plant Science* **14**, 37–42.
- Luan S., Kudla J., Rodriguez-Concepcion M., Yalovsky S. & Gruissem W. (2002) Calmodulins and calcineurin B-like proteins: calcium sensors for specific signal response coupling in plants. *The Plant Cell* **14**, 389–400.
- Ma S., Gong Q. & Bohnert H.J. (2006) Dissecting salt stress pathways. *Journal of Experimental Botany* **57**, 1097–1107.
- Maathuis F.J.M. (2006) The role of monovalent cation transporters in plant responses to salinity. *Journal of Experimental Botany* **57**, 1137–1147.
- Martínez-Atienza J., Jiang X., Garcíadeblas B., Mendoza I., Zhu J.K., Pardo J.M. & Quintero F.J. (2007) Conservation of the SOS salt tolerance pathway. *Plant Physiology* **143**, 1001–1012.
- Mian A., Oomen R.J.F.J., Isayenkov S., Sentenac H., Maathuis F.J.M. & Véry A.-A. (2011) Over-expression of an Na⁺- and K⁺-permeable HKT transporter in barley improves salt tolerance. *The Plant Journal* **68**, 468–479.
- Miller G., Suzuki N., Ciftci-Yimaz S. & Miller R. (2010) Reactive oxygen species homeostasis and signaling during drought and salinity stresses. *Plant, Cell & Environment* **33**, 453–467.
- Møller I.S., Gilliam M., Jha D., Mayo G.M., Roy S.J., Coates J.C., Haseloff J. & Tester M. (2009) Shoot Na⁺ exclusion and increased salinity tolerance engineered by cell type-specific alteration of Na⁺ transport in *Arabidopsis*. *The Plant Cell* **21**, 2163–2178.
- Munns R. & Tester M. (2008) Mechanisms of salinity tolerance. *Annual Review of Plant Biology* **59**, 651–681.
- Murray M.G. & Thompson W.F. (1980) Rapid isolation of high molecular weight plant DNA. *Nucleic Acids Research* **8**, 4321–4325.
- Nevo E. & Chen G.X. (2010) Drought and salt tolerances in wild relatives for wheat and barley improvement. *Plant, Cell & Environment* **33**, 670–685.
- Nieves-Cordones M., Alemán F., Martínez V. & Rubio F. (2010) The *Arabidopsis thaliana* HAK5 K⁺ transporter is required for plant growth and K⁺ acquisition from low K⁺ solutions under saline conditions. *Molecular Plant* **3**, 326–333.
- Oh D.-H., Leidi E., Zhang Q., et al. (2009) Loss of halophytism by interference with SOS1 expression. *Plant Physiology* **151**, 210–222.
- Qiu Q.S., Guo Y., Dietrich M., Schumaker K.S. & Zhu J.K. (2002) Regulation of SOS1, a plasma membrane Na⁺/H⁺ exchanger in *Arabidopsis thaliana*, by SOS2 and SOS3. *Proceedings of the National Academy of Sciences of the United States of America* **99**, 8436–8441.
- Qiu Q.S., Guo Y., Quintero F.J., Pardo J.M., Schumaker K.S. & Zhu J.K. (2004) Regulation of vacuolar Na⁺/H⁺ exchange in *Arabidopsis thaliana* by the salt overly sensitive (SOS) pathway. *The Journal of Biological Chemistry* **279**, 207–215.
- Quan R., Lin H., Mendoza I., Zhang Y., Cao W., Yang Y., Shang M., Chen S., Pardo J.M. & Guo Y. (2007) SCABP8/CBL10, a putative calcium sensor, interacts with the protein kinase SOS2 to protect *Arabidopsis* shoots from salt stress. *The Plant Cell* **19**, 1415–1431.
- Rus A., Lee B.H., Muñoz-Mayor A., Sharkhuu A., Miura K., Zhu J.K., Bressan R.A. & Hasegawa P.M. (2004) AtHKT1 facilitates Na⁺ homeostasis and K⁺ nutrition in planta. *Plant Physiology* **136**, 2500–2511.
- Rushton D.L., Tripathi P., Rabara R.C., et al. (2012) WRKY transcription factors: key components in abscisic acid signaling. *Plant Biotechnology Journal* **10**, 2–11.

- Shabala S. & Cuin T.A. (2007) Potassium transport and plant salt tolerance. *Physiologia Plantarum* **133**, 651–669.
- Shi H., Quintero F.J., Pardo J.M. & Zhu J.K. (2002) The putative plasma membrane Na⁺/H⁺ antiporter SOS1 controls long-distance Na⁺ transport in plants. *The Plant Cell* **14**, 465–477.
- Shi J.R., Kim K.N., Ritz O., Albrecht V., Gupta R., Harter K., Luan S. & Kudla J. (1999) Novel protein kinases associated with calcineurin B-like calcium sensors in *Arabidopsis*. *The Plant Cell* **11**, 2393–2405.
- Soon F.F., Ng L.M., Zhou X.E., *et al.* (2012) Molecular mimicry regulates ABA signaling by SnRK2 kinases and PP2C. *Science* **335**, 85–88.
- Sun J., Chen S.L., Dai S.X., *et al.* (2009) NaCl-induced alternations of cellular and tissue ion fluxes in roots of salt-resistant and salt-sensitive poplar species. *Plant Physiology* **149**, 1141–1153.
- Tamura K., Dudley J., Nei M. & Kumar S. (2007) MEGA4: Molecular Evolutionary Genetics Analysis (MEGA) software version 4.0. *Molecular Biology and Evolution* **24**, 1598–1599.
- Tripathi V., Parasuraman B., Laxmi A. & Chattopadhyay D. (2009) CIPK6, a CBL-interacting protein kinase is required for development and salt tolerance in plants. *The Plant Journal* **58**, 778–790.
- Tsou P.L., Lee S.Y., Allen N.S., Winter-Sederoff H. & Robertson D. (2012) An ER-targeted calcium-binding peptide confers salt and drought tolerance mediated by CIPK6 in *Arabidopsis*. *Planta* **235**, 539–552.
- Verslues P.E., Batelli G., Grillo S., Agius F., Kim Y.S., Zhu J., Agarwal M., Katiyar-Agarwal S. & Zhu J.K. (2007) Interaction of SOS2 with nucleoside diphosphate kinase 2 and catalases reveals a point of connection between salt stress and H₂O₂ signaling in *Arabidopsis thaliana*. *Molecular Cell Biology* **27**, 7771–7780.
- Wang C., Zhang J., Liu X., Li Z., Wu G., Cai J., Flowers T.J. & Wang S. (2009) *Puccinellia tenuiflora* maintains a low Na⁺ level under salinity by limiting unidirectional Na⁺ influx resulting in a high selectivity for K⁺ over Na⁺. *Plant, Cell & Environment* **32**, 486–496.
- Weinl S. & Kudla J. (2009) The CBL-CIPK Ca(2+)-decoding signaling network: function and perspectives. *New Phytologist* **184**, 517–528.
- Xiang Y., Huang Y. & Xiong L. (2007) Characterization of stress-responsive CIPK genes in rice for stress tolerance improvement. *Plant Physiology* **144**, 1416–1428.
- Xu J., Li H.D., Chen L.Q., Wang Y., Liu L.L., He L. & Wu W.H. (2006) A protein kinase, interacting with two calcineurin B-like proteins, regulates K⁺ transporter AKT1 in *Arabidopsis*. *Cell* **125**, 1347–1360.
- Xu L., Jia J., Lv J., Liang X., Han D., Huang L. & Kang Z. (2010) Characterization of the expression profile of a wheat acireductone-dioxygenase-like gene in response to stripe rust pathogen infection and abiotic stresses. *Plant Physiology and Biochemistry* **48**, 461–468.
- Yokoi S., Quintero F.J., Cubero B., Ruiz M.T., Bressan R.A., Hasegawa P.M. & Pardo J.M. (2002) Differential expression and function of *Arabidopsis thaliana* NHX Na⁺/H⁺ antiporters in the salt stress response. *The Plant Journal* **30**, 529–539.
- Zhu J.-K. (2002) Salt and drought stress signal transduction in plants. *Annual Review of Plant Biology* **53**, 247–273.
- Zhu Y., Wang Z., Jing Y.J., Wang L.L., Liu X., Liu Y.X. & Deng X. (2009) Ectopic over-expression of *BhHsf1*, a heat shock factor from the resurrection plant *Boea hygrometrica*, leads to increased thermotolerance and retarded growth in transgenic *Arabidopsis* and tobacco. *Plant Molecular Biology* **71**, 451–467.

Received 11 January 2012; received in revised form 21 March 2012; accepted for publication 22 March 2012

SUPPORTING INFORMATION

Additional Supporting Information may be found in the online version of this article:

Table S1. Primers used in the paper.

Table S2. Gene products of annotated genes at least twofold change in transcript abundance ($P < 0.05$) in HbCIPK2-overexpressing line W116 compared with WT plants in non-saline condition.

Table S3. Gene products of annotated genes at least twofold change in transcript abundance ($P < 0.05$) in HbCIPK2-overexpressing line W116 compared with WT plants in saline condition.

Please note: Wiley-Blackwell are not responsible for the content or functionality of any supporting materials supplied by the authors. Any queries (other than missing material) should be directed to the corresponding author for the article.